British Journal of Pharmacology

DOI:10.1111/bph.12012
www.brjpharmacol.org

RESEARCH PAPER

Sphingosine and FTY720 are potent inhibitors of the transient receptor potential melastatin 7 (TRPM7) channels

Correspondence
Dr Lixia Yue, University of Connecticut Health Center, 263 Farmington Ave., Farmington, CT 06030, USA. E-mail: lyue@uchc.edu

Keywords
TRPM7; sphingosine; FTY720; TRP channels; cardiac fibroblasts

Received
29 April 2012
Revised
30 September 2012
Accepted
2 October 2012

Xin Qin[1,2], Zhichao Yue[1], Baonan Sun[1], Wenzhong Yang[1], Jia Xie[1], Eric Ni[1], Yi Feng[1], Rafat Mahmood[1], Yanhui Zhang[1] and Lixia Yue[1]

[1]*Calhoun Cardiology Center, Department of Cell Biology, University of Connecticut Health Center, Farmington, CT, USA, and* [2]*Department of Physiology, College of Basic Medical Sciences, China Medical University, Shenyang, China*

BACKGROUND AND PURPOSE

Transient receptor potential melastatin 7 (TRPM7) is a unique channel kinase which is crucial for various physiological functions. However, the mechanism by which TRPM7 is gated and modulated is not fully understood. To better understand how modulation of TRPM7 may impact biological processes, we investigated if TRPM7 can be regulated by the phospholipids sphingosine (SPH) and sphingosine-1-phosphate (S1P), two potent bioactive sphingolipids that mediate a variety of physiological functions. Moreover, we also tested the effects of the structural analogues of SPH, N,N-dimethyl-D-erythro-sphingosine (DMS), ceramides and FTY720 on TRPM7.

EXPERIMENTAL APPROACH

HEK293 cells stably expressing TRPM7 were used for whole-cell, single-channel and macropatch current recordings. Cardiac fibroblasts were used for native TRPM7 current recording.

KEY RESULTS

SPH potently inhibited TRPM7 in a concentration-dependent manner, whereas S1P and other ceramides did not produce noticeable effects. DMS also markedly inhibited TRPM7. Moreover, FTY720, an immunosuppressant and the first oral drug for treatment of multiple sclerosis, inhibited TRPM7 with a similar potency to that of SPH. In contrast, FTY720-P has no effect on TRPM7. It appears that SPH and FTY720 inhibit TRPM7 by reducing channel open probability. Furthermore, endogenous TRPM7 in cardiac fibroblasts was markedly inhibited by SPH, DMS and FTY720.

CONCLUSIONS AND IMPLICATIONS

This is the first study demonstrating that SPH and FTY720 are potent inhibitors of TRPM7. Our results not only provide a new modulation mechanism of TRPM7, but also suggest that TRPM7 may serve as a direct target of SPH and FTY720, thereby mediating S1P-independent physiological/pathological functions of SPH and FTY720.

LINKED ARTICLE

This article is commented on by Rohacs, pp. 1291–1293 of this issue. To view this commentary visit http://dx.doi.org/10.1111/bph.12070

Abbreviations

FTY720, fingolimod, 2-amino-2-propane-1,3-diol hydrochloride; FTY720-P, FTY720-phosphate; S1P, sphingosine-1-phosphate; SPH, sphingosine; TRPM7, transient receptor potential melastatin 7

Introduction

The transient receptor potential melastatin 7 (TRPM7) is a unique channel kinase (Nadler *et al.*, 2001; Runnels *et al.*, 2001; Yamaguchi *et al.*, 2001) which exerts a variety of physiological/pathological functions, including cellular Mg^{2+} homeostasis (Schmitz *et al.*, 2003), anoxia/ischaemia-induced neuronal cell death (Aarts *et al.*, 2003; Sun *et al.*, 2009), early

embryonic development (Jin *et al.*, 2008; Ryazanova *et al.*, 2010; Jin *et al.*, 2012; Liu *et al.*, 2011), fibrosis-associated atrial fibrillation (AF) (Du *et al.*, 2010), breast tumour cell metastasis (Middelbeek *et al.*, 2012) and various other cellular functions (Elizondo *et al.*, 2005; McNeill *et al.*, 2007; Sahni *et al.*, 2010; Bates-Withers and Sah, 2012). TRPM7 is ubiquitously expressed in various cells and tissues, and is markedly up-regulated under pathological conditions (Sun *et al.*, 2009; Du *et al.*, 2010).

Although the importance of its physiological/pathological functions has been highly appreciated, how TRPM7 is activated and inactivated under physiological/pathological conditions is not fully understood. At physiological intracellular Mg^{2+} concentrations, TRPM7 is constitutively active to a small degree. The channel activity of TRPM7 is inhibited by depletion of PIP_2 upon activation of PLC through G_q-linked receptor stimulation (Runnels *et al.*, 2002; Xie *et al.*, 2011). PIP_2 seems to control the gating of TRPM7, as mutations of the putative PIP_2-binding sites result in non-functional TRPM7 channels (Xie *et al.*, 2011). Whereas PIP_2 is required for TRPM7 channel activity (Runnels *et al.*, 2002; Kozak *et al.*, 2005; Gwanyanya *et al.*, 2006; Xie *et al.*, 2011), intracellular Mg^{2+}, Mg^{2+}-ATP, polyvalent cations and protons inhibit TRPM7 (Kerschbaum *et al.*, 2003; Kozak *et al.*, 2005; Demeuse *et al.*, 2006). Pathological conditions drastically up-regulate TRPM7 expression (Sun *et al.*, 2009; Du *et al.*, 2010). For example, TRPM7 current amplitude was increased by three- to fivefold in cardiac fibroblasts isolated from AF patients (Du *et al.*, 2010). Moreover, although it is not clear what activates TRPM7, acidic extracellular conditions remarkably potentiate TRPM7 inward currents by releasing divalent block on inward TRPM7 monovalent currents, making TRPM7 a monovalent selective channel which can induce depolarization under ischaemic pathological conditions (Jiang *et al.*, 2005; Li *et al.*, 2007). Given its unique properties and important physiological/pathological functions, TRPM7 could be an effective therapeutic target under various pathological conditions. Thus, it is important to understand how TRPM7 is regulated *in vivo*, and to identify TRPM7 specific blockers. Recent studies have demonstrated that TRPM7 can be modulated by various reagents. A non-specific modulator of several TRP channels, 2-APB inhibits endogenous TRPM7 (Prakriya and Lewis, 2002) and heterologously expressed TRPM7 currents (Li *et al.*, 2006) but potentiates TRPM6 currents at micromolar concentrations. Thus, 2-APB can be used to distinguish TRPM6 and TRPM7 currents. TRPM7 is also blocked by carvacrol (Parnas *et al.*, 2009), 5-lipoxygenase inhibitors (Chen *et al.*, 2010a), a synthetic serine protease inhibitor nafamostat mesylate (Chen *et al.*, 2010b) and Ca^{2+}-activated small conductance K^+ channel blocker NS8593 (Chubanov *et al.*, 2012). A recent study demonstrated that Waixenicin A extracted from soft coral potently and specifically blocks TRPM7 in a Mg^{2+}-dependent manner (Zierler *et al.*, 2011). Future studies will provide more information as to whether these exogenous modulators of TRPM7 are useful tools for investigating how manipulation of TRPM7 channel activity may achieve therapeutic purpose.

As TRPM7 is involved in various cellular processes and physiological functions, to further understand how TRPM7 is modulated *in vivo* and exerts its potential physiological/pathological functions, we investigated the effects of two bioactive sphingolipids, sphingosine (SPH) and its phosphorylated form sphingosine-1-phosphate (S1P), on TRPM7 currents over-expressed in HEK293 cells and on endogenous TRPM7 currents in cardiac fibroblasts. SPH and S1P are potent bioactive sphingolipids which are associated with a vast number of cellular and biological processes such as cell survival, apoptosis, senescence, differentiation, proliferation, mitogenesis, inflammation and angiogenesis (Hannun and Obeid, 2008; Pyne and Pyne, 2010). SPH is a metabolite generated during the de novo synthesis of cellular sphingolipids (Hannun *et al.*, 2001), and is converted to S1P by sphingosine kinase 1 (SK1) and 2 (SK2). S1P activates a family of five G protein-coupled receptors, S1PR1-5 (Hannun and Obeid, 2008; Pyne and Pyne, 2010), leading to biological responses such as proliferation, inflammation, migration and angiogenesis. In addition to activation of S1PRs when converted to S1P, SPH also has its own targets, such as PKC and phospholipase A2 (Hannun *et al.*, 1986; Pyne and Pyne, 2010). The synthetic sphingosine analogue FTY720 has been used as an immunosuppressant, and has been recently approved by the U.S. Food and Drug Administration (FDA) as the first oral drug for multiple sclerosis (Brinkmann *et al.*, 2010; Chun and Brinkmann, 2011). FTY-720 is phosphorylated *in vivo* by SK2 (Zemann *et al.*, 2006), and the phosphorylated FTY720-P binds to S1P receptor (Hannun and Obeid, 2008), causing aberrant internalization of S1PR1 in T cells (Pham *et al.*, 2008; Grigorova *et al.*, 2009), thereby preventing their egress from the lymph (Mandala *et al.*, 2002). Although the clinical efficacy of FTY720 has been assumed to be mediated by its phosphorylated form FTY720-P, recent studies have demonstrated that some effects of FTY720, such as its anti-tumour effects, are independent of S1P receptor signalling pathways (Azuma *et al.*, 2003a,b; Pitman *et al.*, 2012). FTY720, but not FTY720-P, is anti-proliferative in breast and colon cancer *in vitro* (Nagaoka *et al.*, 2008). Moreover, FTY720 has other biological functions that are distinct from those of FTY720-P (Pyne and Pyne, 2010). For example, FTY720 inhibits phospholipase A2 (Pyne and Pyne, 2010), sphingosine-1-phosphate lyase (SGPL1) (Bandhuvula *et al.*, 2005), SK1 (Vessey *et al.*, 2007), and ceramide synthesis (Lahiri *et al.*, 2009), and activates PP2A and PP2A-like phosphatases (Neviani *et al.*, 2007; Berdyshev *et al.*, 2009). FTY720 has exhibited both *in vivo* and *in vitro* functions independent of S1P receptors (Pyne and Pyne, 2010). Therefore, in addition to the functions mediated by S1PRs, FTY720 may exert physiological, pathological and therapeutic functions through its own targets.

A previous study has demonstrated that SPH activates TRPM3 (Grimm *et al.*, 2005) without activating several other TRP channels. We report here that SPH, but not S1P, is a potent inhibitor of TRPM7. The structural analogues of SPH, N,N-dimethyl-D-erythro-sphingosine (DMS) but not ceramides, also markedly inhibit TRPM7. Whereas FTY720 inhibits TRPM7 with similar potency to SPH, FTY720-P does not have any effect. We demonstrated that SPH and FTY720 efficiently inhibit TRPM7 by reducing single-channel open probability in excised inside-out patches, suggesting that SPH and FTY720 block TRPM7 channel activity independent of intracellular signalling molecules and pathways. Furthermore, we found that SPH also strongly blocks TRPM6, but not other TRPM channels such as TRPM2 and TRPM4. Although both TRPM6 and TRPM7 are potently blocked by SPH, given that

TRPM7 is ubiquitously expressed whereas TRPM6 is limited in intestine and kidney, it is likely that TRPM7 may serve as a direct target of SPH and FTY720. Taken together, our results not only provide a new endogenous modulation mechanism of TRPM7, but also suggest that TRPM7 is a direct target of SPH and FTY720, which may contribute to the S1PR-independent physiological, pathological or therapeutic functions of SPH and FTY720.

Methods

Chemicals

D-erythro-sphingosine (SPH) and D-erythro-sphingosine-1-phosphate (S1P) were purchased from Sigma (St. Louis, MO, USA), whereas DMS, N-acetyl-D-erythro-sphingosine (C2-Cer), N-octanoyl-D-erythro-sphingosine (C8-Cer), FTY720 and FTY720-phosphate were obtained from Cayman Chemicals (Ann Arbor, MI, USA). All the stock solutions were prepared and stored according to the suppliers' instructions. The chemicals were dissolved in Tyrode solution to their final concentrations right before they were used to perfuse the cells.

Cell culture and transfection

A description and characterization of the 293-TRPM7 cell line expressing hemagglutinin (HA)-tagged murine TRPM7 (GenBank Accession No. AF376052) was previously described (Jiang *et al.*, 2005). The over-expression of HA-tagged TRPM7 in 293-TRPM7 cell was induced by the addition of tetracycline (1 $mg{\cdot}mL^{-1}$) to the growth medium. Cells were grown in DMEM/Ham's F-12 medium supplemented with 10% FBS, 100 $U{\cdot}mL^{-1}$ penicillin, and 100 $mg{\cdot}mL^{-1}$ streptomycin at 37°C in a humidity-controlled incubator with 5% CO_2.

TRPM2 and TRPM4 were transiently transfected into HEK-293 cells for whole-cell current recordings as we previously reported (Li *et al.*, 2007; Du *et al.*, 2009b). As HEK-293 cells express endogenous TRPM7 currents with an amplitude of 300–500 pA (Li *et al.*, 2007), we transfected TRPM6 plasmids into CHOK1 cells for current recording in order to minimize the influence of TRPM7 on TRPM6 currents (Li *et al.*, 2006).

Human cardiac tissue sample collection

Myocardial samples of the right atria were collected during cardiac surgery. All procedures involving human tissue use were approved by the institutional review boards of the University of Connecticut Health Center. Consent was obtained from patients before tissue harvest. Atrial samples were obtained from normal sinus rhythm patients (Du *et al.*, 2010). On excision, the samples were immediately placed in cold and oxygenated nominally calcium-free HBSS solution for transport to the laboratory.

Isolation of cardiac fibroblasts from human atrial samples and mouse heart

All studies involving animals are reported in accordance with the ARRIVE guidelines for reporting experiments involving animals (Kilkenny *et al.*, 2010; McGrath *et al.*, 2010). Atrial samples were minced and incubated in collagenase (150–200 $U{\cdot}mL^{-1}$ CLS II, Worthington Biochemical, Freehold, NJ, USA, 300 $U{\cdot}mg^{-1}$) in a shaking water bath at 37°C. Isolated cells were harvested after each 10 min digestion period. After five digestion periods, all isolated cells were then centrifuged at 830 *g* for 10 min. Fibroblasts were re-suspended and cultured in DMEM media containing 10% FBS, or used freshly for patch-clamp experiments (Du *et al.*, 2010). Mouse cardiac fibroblasts were isolated using the same method. The cell capacitance of human and mouse fibroblasts was between 4 and 8 pF. All procedures used in handling mice were approved by the Animal Care Committee at the University of Connecticut Health Center in compliance with the Animal Welfare Assurance.

Electrophysiological recordings

Whole-cell currents of TRPM7 were recorded using an Axopatch 200B amplifier. Data were digitized at 5 or 10 kHz, and digitally filtered off-line at 1 kHz. Patch electrodes were pulled from borosilicate glass and fire polished to a resistance of 3–5 MΩ when filled with internal solutions for whole-cell current recordings. Series resistance (Rs) was compensated up to 90% to reduce series resistance errors to <5 mV. Cells with Rs bigger than 10 MΩ were discarded. All patch-clamp experiments were performed at room temperature (20–25°C).

Whole-cell current recording was described in a previous report (Jiang *et al.*, 2005). Voltage stimuli lasting for 250 ms were delivered at 1 s intervals, with voltage ramps ranging from −120 to +100 mV. A fast perfusion system was used to exchange extracellular solutions, with complete solution exchange achieved in about 1–3 s. Cells were perfused with Tyrode solution before and after application of each compound. Unless otherwise stated, each compound was diluted from the stock solution to the external Tyrode solution and applied to the cells after TRPM7 current reached steady state. Compounds were washed out by Tyrode solution once the maximal effect was observed. The internal pipette solution for TRPM7 whole-cell current recordings contained (in mM) 145 Cs-methanesulfonate ($CsSO_3CH_3$), 8 NaCl, 10 EGTA, and 10 HEPES, with pH adjusted to 7.2 with CsOH. The standard extracellular Tyrode's solution for whole-cell recording contained (mM): 145 NaCl, 5 KCl, 2 $CaCl_2$, 10 HEPES and 10 glucose; pH was adjusted to 7.4 with NaOH.

The pipette solution and extracellular solution for TRPM6 current recordings were the same as those used for TRPM7 current recording (Li *et al.*, 2006). For TRPM2 current recording, 200 μM and 10 μM Ca^{2+} were included in the pipette solution (Du *et al.*, 2009b). For the current recording of TRPM4, 100 μM free Ca^{2+} was included in the pipette solution (Li *et al.*, 2007).

Single-channel currents were recorded in inside-out patches as previously described (Du *et al.*, 2009a; 2010). Divalent-free (DVF) solution was used in both internal and external sides of the patches. The pipette solution contained (mM): 140 $NaSO_3CH_3$, 8 NaCl, 10 HEPES, 10 EGTA, 2 EDTA and 10 glucose (pH 7.4 adjusted with NaOH); and the bath solution contained (mM): 140 $NaSO_3CH_3$, 8 NaCl, 10 EGTA, 2 EDTA and 10 HEPES (pH 7.2 adjusted with NaOH). Chemicals were diluted in the DVF perfusion solution from the stock solutions for the inside-out excised patch experiments. The pipette resistance for single-channel recordings was 8–10 MΩ.

For currents recorded from macropatches, pipette solution (extracellular solution) contained (mM): 145 NaCl, 5 KCl, 2 $CaCl_2$, 10 HEPES and 10 glucose; pH was adjusted to

7.4 with NaOH; and the DVF bath solution (intracellular solution) contained (mM): 140 $NaSO_3CH_3$, 8 NaCl, 10 EGTA, 2 EDTA and 10 HEPES (pH 7.2 adjusted with NaOH). Experiments were conducted using pipette with resistance between 2 and 3 MΩ.

Data analysis

Data were analysed using Clampfit 9.0 (Axon Instruments, Union City, CA, USA) and GraphPad Prism (GraphPad Software, Inc., La Jolla, CA, USA). Averaged data are presented as mean ± SE. Dose–response curves were fitted by an equation of the form $E = E_{max}\{1/[1 + (EC_{50}/C)^n]\}$, where E is the effect at concentration C, E_{max} is the maximal effect, EC_{50} is the concentration for half-maximal effect, and n is the Hill coefficient (Jiang *et al.*, 2005). EC_{50} is replaced by IC_{50} if the effect is an inhibitory effect. Statistical comparisons were made using two-way ANOVA and two-tailed *t*-test with Bonferroni correction; $P < 0.05$ indicated statistical significance.

Results

SPH is a potent endogenous inhibitor of TRPM7

TRPM7 exhibits various physiological/pathological functions including embryonic development (Jin *et al.*, 2008; Ryazanova *et al.* 2010; Liu *et al.* 2011), neuronal cell death (Aarts *et al.*, 2003), fibroblast differentiation (Du *et al.*, 2010) and many other biological functions (Elizondo *et al.*, 2005; McNeill *et al.*, 2007; Sahni *et al.*, 2010). In order to understand how TRPM7 is regulated *in vivo*, we tested if SPH, an active endogenous bioactive phospholipid, has any effect on TRPM7. As shown in Figure 1, currents were elicited in HEK-293 cells stably expressing TRPM7 by a ramp protocol ranging from –100 to +100 mV (Figure 1A). Cells were perfused with Tyrode solution before and after being exposed to the tested compounds. Extracellular application of SPH at various concentrations significantly inhibited outward currents (Figure 1A) and inward currents (Figure 1B) in a concentration-dependent manner. Because TRPM7 is a strong outward-rectifying channel, and the inward current amplitude is usually one-tenth to one-fiftieth of the outward current amplitude, we enlarged the y-axis to show changes of inward currents in Figure 1B. The time-dependent changes of outward and inward currents in representative cells exposed to 0.5 and 1 μM SPH are illustrated in Figure 1C,D. The inward and outward currents were inhibited in parallel, and the effect of SPH on TRPM7 was reversible, albeit the reversal process was slow (Figure 1C,D). At 0.5 μM SPH, the time course for inhibition was slower than that of 1 μM SPH, whereas recovery from 1 μM SPH blockade took a much longer time than that of 0.5 μM. Because the time course is too long to see the onset of the blockade (Figure 1D), a graph with an enlarged x-axis of Figure 1D is shown in Supporting Information Fig. S1. The rapid block at high concentrations of SPH is obvious as shown in the panel with the superimposed time course (Supporting Information Fig. S1B).

Although it seems that the inward and outward currents were blocked in parallel (Figure 1C,D), we analysed whether there was a voltage-dependent block as we previously reported (Li *et al.*, 2006). As shown in Figure 1E, the percentage inhibition of 1 μM SPH at all the tested voltages was similar. For example, there was 98.2 ± 7.8%, 97.5 ± 9.8%, 98.8 ± 8.78%, 99.2 ± 9/68% inhibition at –100, –40, +40 and +100 mV, respectively (inset of Figure 1E), and no statistical difference in the inhibition was observed at the tested voltages. Because the effects of SPH were non-voltage dependent, we used the current amplitude measured at +100 mV to evaluate the blockade of SPH. The inhibitory effect of SPH at various concentrations is shown in Figure 1F, and the IC_{50} obtained by the best fit of the dose–response curve was 0.59 μM (Figure 1F). The effect of SPH on TRPM7 seems to be independent of the kinase domain of TRPM7, because the kinase truncation mutant of TRPM7 was equally blocked by SPH (Supporting Information Fig. S2).

SPH is one of the endogenous active phospholipids in the sphingolipid pathway. There are several structurally related analogues (Figure 2). Because SPH is generated by the conversion of ceramide, we next tested if the precursor ceramide has any effect on TRPM7. As shown in Figure 3, neither C2-Ceramide nor C8-Ceramide produced significant effect on TRPM7 current amplitude at the concentrations of up to 10 μM (Figure 3). Concentrations higher than 10 μM were not tested. These results indicate that ceramides at a concentration 10-fold higher than the IC_{50} of SPH have no effects on TRPM7.

SPH can be further phosphorylated *in vivo* by sphingosine kinases 1 and 2 (SphK 1, SphK 2) to produce sphingosine-1-phosphate (S1P), a potent bioactive lipid that activates S1P receptors and exhibits a broad spectrum of biological activities including cell proliferation, survival, migration, cytoskeletal organization and morphogenesis. Thus, we determined to test whether S1P could directly inhibit TRPM7 activity. As shown in Figure 3E,F, S1P at 10 μM failed to produce any noticeable effects on TRPM7 over-expressed in HEK-293 cells, indicating that SPH, but not its phosphorylated form S1P, is a potent inhibitor of TRPM7.

Structurally related analogue of SPH strongly inhibited TRPM7

The inhibitory effects of SPH, but not S1P or ceramides, on TRPM7 suggest that there might be a structure requirement for SPH to block TRPM7. Therefore, we tested the effects of other structurally related analogues of SPH on TRPM7 (Figure 2). DMS is a competitive inhibitor of sphingosine kinase. Interestingly, we found that DMS completely blocked TRPM7 currents at 1 μM (Figure 4). Both inward and outward currents of TRPM7 were efficiently inhibited by DMS (Figure 4B,C). The IC_{50} obtained from the best fit of the concentration-dependent curve was 0.3 μM, similar to the IC_{50} of SPH on TRPM7.

Effects of FTY720 and FTY720-P on TRPM7

We next tested whether FTY720 inhibits TRPM7 channel activity. FTY720 (Fingolimod) is a structural analogue of sphingosine. It is a derivative of myriocin (ISP-1), a fungal metabolite of the Chinese herb *Isaria sinclairii*. FTY720 is a novel immunosuppressive drug investigated in clinical trials for organ transplantation and has been approved by the FDA (USA) for multiple sclerosis. Because of its structural analogy with the naturally occurring lipid sphingosine, cells take up

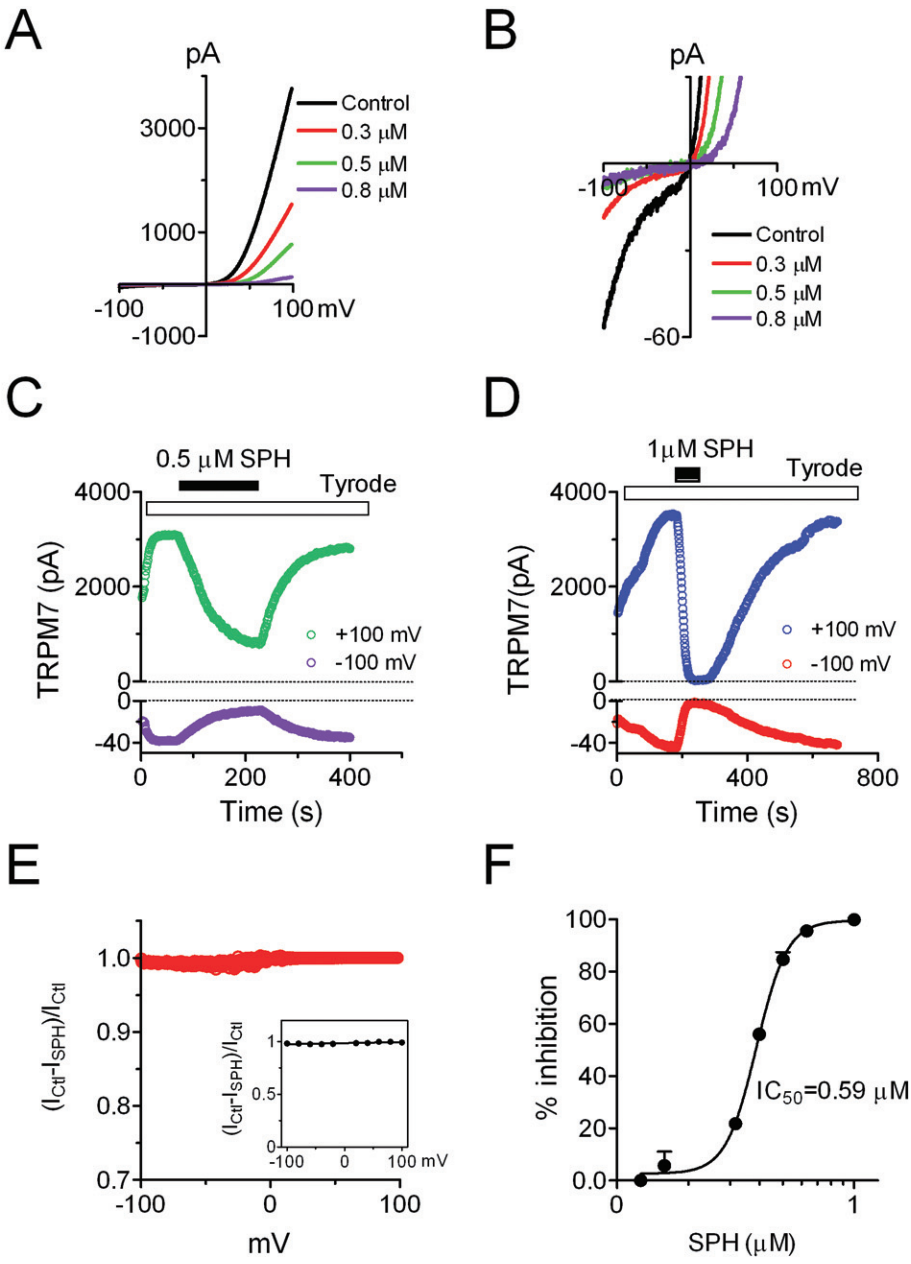

Figure 1

Effects of SPH on TRPM7 whole-cell currents recorded in HEK-293 cells over-expressing TRPM7. Cells were perfused with Tyrode solution before and after exposure to SPH. Currents were elicited by a ramp protocol ranging from –100 to +100 mV. (A) Representative recordings of TRPM7 in the absence and presence of SPH at 0.3, 0.5 and 0.8 μM. Note the large outward current and small inward current, a feature of outward-rectifying TRPM7. (B) Illustration of changes of inward currents with enlarged y-axis for the recordings shown in (A). Note the inhibition of TRPM7 inward currents by 0.3, 0.5 and 0.8 μM SPH. (C) Time-dependent changes of TRPM7 outward current measured at +100 mV and inward current measured at –100 mV before and after 0.5 μM SPH. (D) Time-dependent changes of TRPM7 outward and inward currents before and after 1 μM SPH. Note the slow recovery of TRPM7 after being completely blocked by 1 μM SPH. (E) Analysis of voltage-dependent effects of SPH on TRPM7. The inhibitory effects at all the tested voltages were calculated by subtracting a TRPM7 control trace (Ctl) from a trace recorded after 1 μM SPH, and then dividing by the Ctl trace: Inhibition = $(I_{Ctl}–I_{SPH})/I_{Ctl}$. Data points at 0 mV were not included in the 'E'. Note that the inhibitory effects at all the voltages are similar. Inset: average inhibition at –100, –80, –60, –40, –20, +20, +40, +60, +80 and +100 mV, respectively (n = 6). No statistical difference was observed. (F) Concentration-dependent effects of SPH on TRPM7. The best fit of dose–response curve yielded IC_{50} = 0.59 ± 0.02 μM (n = 6 at each concentration).

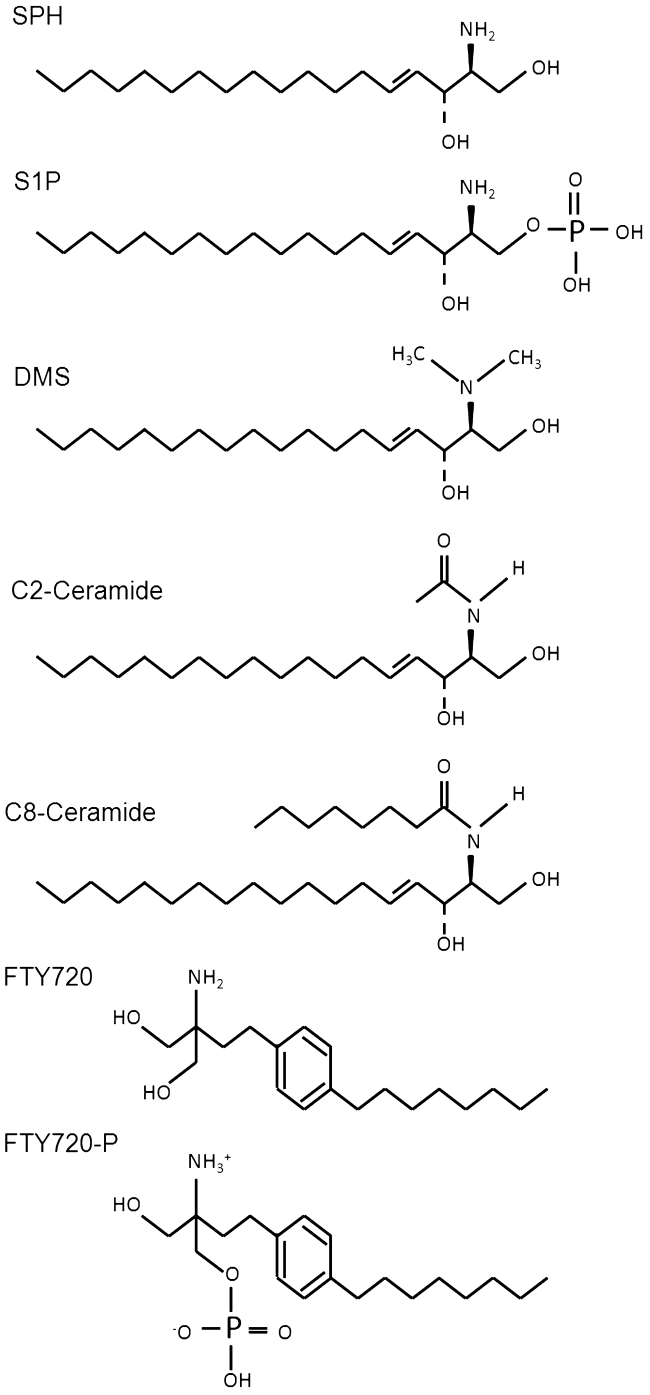

Figure 2

Chemical structure of SPH analogues. SPH: D-erythro-sphingosine; S1P: D-erythro-sphingosine-1-phosphate; DMS: N,N-dimethyl-D-erythro-sphingosine; C2-Cer: N-acetyl-D-erythro-sphingosine; C8-Cer: N-octanoyl-D-erythro-sphingosine; FTY720: 2-amino-2-propane-1,3-diol hydrochloride; FTY720-P: 2-amino-2[2-(4-octylphenyl)ethyl]-1,3-propanediol, mono dihydrogen phosphate ester.

FTY720 and phosphorylate it to its bioactive form, FTY720-P. We tested the effect of both FTY720 and FTY720-P on TRPM7 whole-cell currents recorded in over-expressing HEK293 cells. As shown in Figure 5, FTY720 was applied to the cell when TRPM7 current reached a steady state. At 1 μM, FTY720 blocked TRPM7 by 100% (Figure 5A,B). After washout, TRPM7 currents were slowly but fully recovered (Figure 5B). As both inward and outward currents were blocked, we used current amplitudes measured at +100 mV to evaluate the blockade effects. TRPM7 was inhibited in a concentration-dependent manner (Figure 5C), and the IC_{50} obtained by the best fit of the dose–response curve was 0.72 μM (Figure 5D). In contrast to FTY720, 1 μM FTY720-P did not produce any inhibition on TRPM7 (data not shown), and 10 μM FTY720-P did not produce any noticeable change to TRPM7 current either (Figure 5E,F). Therefore, FTY720, but not its phosphorylated form, is a strong inhibitor of TRPM7.

Effects of SPH on single-channel properties of TRPM7

To understand the mechanism by which SPH or FTY720 inhibits TRPM7, we utilized inside-out excised patches to investigate how SPH may influence single-channel properties of TRPM7. As shown in Figure 6, single-channel currents were recorded by using DVF solution in the pipette and in the perfusion solution (Figure 6A). Single-channel conductance calculated by linear regression of the current amplitudes at various voltages was 38.3 ± 0.9 pS, similar to the conductance recorded in the CHOK cells over-expressing TRPM7 (Li *et al.*, 2006). We next tested the effects of SPH on the single-channel currents. In the patches where multiple channels were present, application of 3 μM SPH efficiently closed the channel openings (Figure 7B). However, single-channel current amplitude was not changed, suggesting that single-channel conductance was not changed by SPH. The effect of SPH was reversible upon washout. The effects of 3 μM SPH is similar to the effects produced by 50 μM $MgCl_2$. The average NP_o was reduced from 2.95 ± 0.7 to 0.3 ± 0.16 by 3 μM SPH (Figure 6D), consistent with the inhibitory effect of SPH on the whole-cell currents. These results indicate that SPH is a potent blocker which inhibits TRPM7 channel activity by reducing the open probability without changing single-channel conductance.

The effects of SPH on TRPM7 single-channel currents recorded in inside-out patches suggest that SPH can block TRPM7 in the absence of other intracellular signalling components. We further tested this notion by determining whether SPH can block TRPM7 currents recorded using macropatch. As shown in Figure 7A, currents were recorded using the ramp protocol ranging from −100 to +100 mV. SPH at 1 μM effectively inhibited TRPM7 current, and this effect was reversible and reproducible (Figure 7A,B). SPH at 1 μM inhibited TRPM7 macropatch currents by 96.7% (Figure 7C), consistent with the results from the whole-cell recordings (Figure 1). These results indicate that SPH is able to block TRPM7 channel activity independent of intracellular signalling molecules or pathways.

Effects of SPH on endogenous TRPM7 current in cardiac fibroblasts

To investigate whether SPH blocks endogenous TRPM7 currents, we tested the effects of SPH, DMS and FTY720 on TRPM7 currents in cardiac fibroblasts isolated from human atrium. As we previously reported, TRPM7 is highly expressed in cardiac fibroblasts and TRPM7 currents can be readily

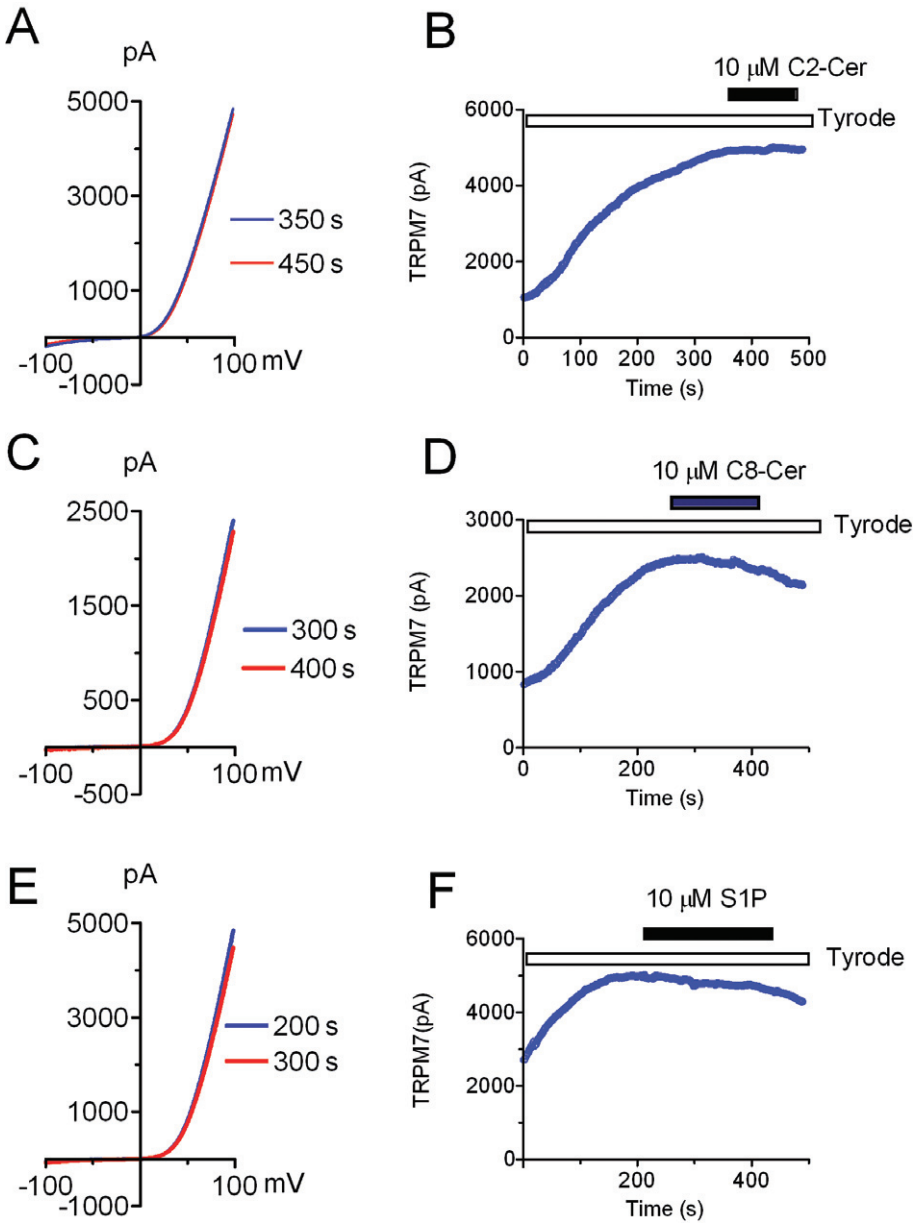

Figure 3

Effects of C2-Cer, C8-Cer and S1P on TRPM7 whole-cell currents. (A, C, E) Representative recordings of TRPM7 recorded in HEK-293 cells over-expressing TRPM7 before and after application of 10 μM C2-Cer (A), C8-Cer (C) and S1P (E). (B, D, F) Time-dependent changes of outward current amplitude measured at +100 mV before and after 10 μM C2-Cer (B), C8-Cer (D) and S1P (F). There was no noticeable change observed after application of C2-Cer, C8-Cer or S1P (n = 5 cells were tested for each compound).

recorded in cardiac fibroblasts (Du *et al.*, 2010). As the closest homologue of TRPM7, TRPM6 was barely detectable at RNA level in fibroblasts (Du *et al.*, 2010), and there is no report demonstrating functional expression of TRPM6 in cardiac fibroblasts so far. Moreover, TRPM7 shRNA was able to knock down the outward-rectifying currents in fibroblasts, indicating that TRPM7 encodes the outward-rectifying current in cardiac fibroblasts (Du *et al.*, 2010). Using the same ramp protocol as we used previously (Du *et al.*, 2010), TRPM7 currents were readily recorded in human cardiac fibroblasts (Figure 8). SPH was applied to the cells when TRPM7 current amplitude reached a steady state (Figure 8B). SPH at 1 μM completely inhibited TRPM7 currents. Like SPH, DMS and FTY720 also fully inhibited TRPM7 currents recorded in human atrial fibroblasts at 1 μM (Figure 8). Similar effects of SPH and FTY720 were also observed in mouse cardiac fibroblasts (Figure 9).

Effects of FTY720 on motility and proliferation

In order to investigate whether blocking TRPM7 by SPH, FTY720 and DMS will influence TRPM7-dependent cellular

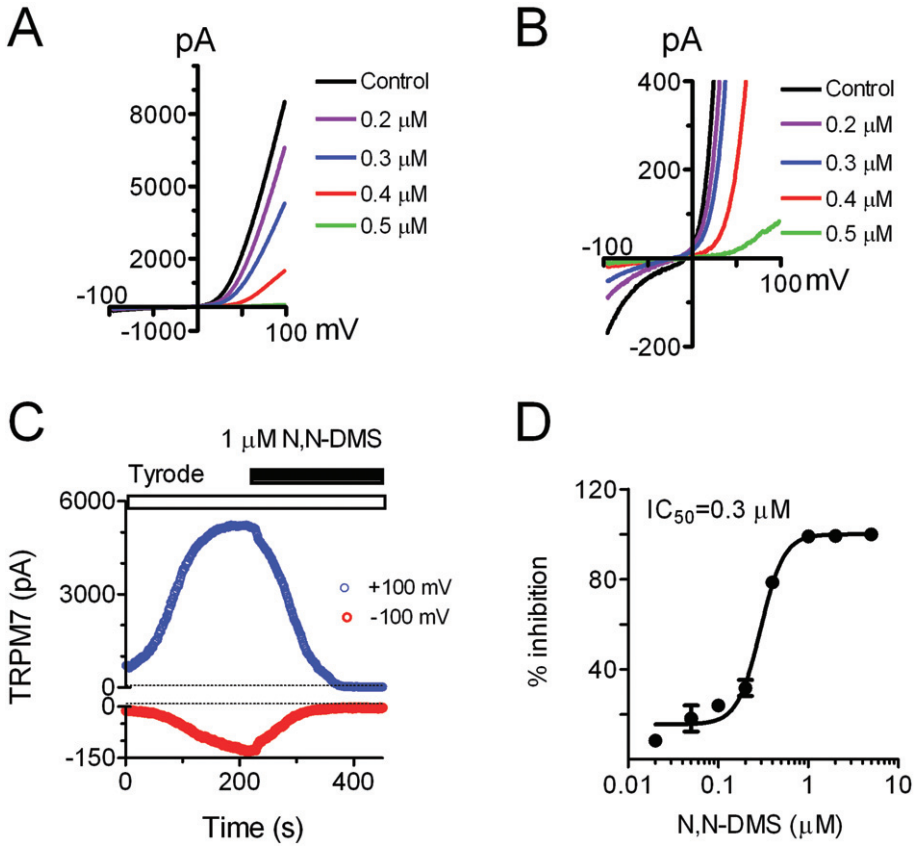

Figure 4

DSM potently inhibited TRPM7 channel activity in whole-cell current recordings in the over-expressing HEK-293 cells. (A) Representative recordings of TRPM7 in the absence and presence of 0.3, 0.5 and 0.8 μM DMS. Cells were perfused with Tyrode solution before and after exposure to DMS. (B) Changes of inward currents by DMS using an enlarged y-axis. (C) Time-dependent changes of TRPM7 outward current measured at +100 mV and inward current measured at –100 mV before and after 1 μM DMS. (D) Concentration-dependent effects of DSM on TRPM7. The inhibition effects were evaluated using the current amplitude measured at +100 mV. The best fit of dose–response curve yielded IC_{50} = 0.59 ± 0.02 μM (n = 6).

functions, we tested the effects of FTY720 on motility and proliferation properties of the HEK-293. We used HEK-293 cells because they lack S1P receptors (Lee *et al.*, 1998; Molderings *et al.*, 2007), therefore excluding any effect mediated by S1P receptors. Moreover, FTY720 is not converted to FTY720-P in HEK-293 cells (Lahiri *et al.*, 2009). Thus, we chose FTY720 and FTY720-P for the experiments. As over-expressing of TRPM7 at high level can cause cell rounding and detachment (Su *et al.*, 2006), we used HEK-293 cells without induction of TRPM7 over-expression, as Chubanov and colleague reported recently (Chubanov *et al.*, 2012). Although it was apparent that FTY720 can block endogenous TRPM7 currents in human fibroblasts (Figure 8) and can inhibit TRPM7 current in HEK-293 cells to almost 100% (Figure 1E), to ensure that FTY720 is a potent blocker of endogenous TRPM7 currents in HEK293 cells, we recorded endogenous TRPM7 currents and tested the effects of FTY720. We found that the endogenous TRPM7 current in HEK-293 cells can be efficiently blocked by FTY720. At 1 μM FTY720, endogenous TRPM7 in HEK-293 cells was reduced from 357.4 ± 23.8 pA to 13.9 ± 3.7 pA (measured at +100 mV, n = 6, P < 0.001). We then went on to use a wound healing assay to evaluate the motility of the cells. As shown in Figure 10, cells treated with FTY720 for 24 h exhibited significantly reduced wound closure speed in comparison to the mock-treated cells (Ctl), and FTY720-P-treated cells (Figure 10A–C), suggesting that blocking TRPM7 inhibits cell motility. For the proliferation experiments, a statistical significant difference was not observed after 24 h treatment. Cell number was 34 ± 1.9, 40.3 ± 1.5 and 39.6 ± 1.6 million per dish in mock-treated (Ctl), FTY720-treated and FTY720-P-treated groups, respectively. However, a statistical difference was obtained after 48 h treatment as shown in Figure 10D, indicating that blocking TRPM7 by FTY720 alters cell proliferation properties.

Effects of SPH on other TRP channels

SPH has been demonstrated to activate TRPM3 at micromolar concentration without activating other TRP channels such as TRPM2 (Grimm *et al.*, 2005). We next tested whether SPH exerts inhibitory effects on the other TRPM channels including TRPM2, TRPM4 and TRPM6. As shown in Figure 11A,B, TRPM2 currents were activated by 200 μM ADPR and 10 μM Ca^{2+} included in the pipette solution as we previously reported (Du *et al.*, 2009a). SPH at 10 μM did not produce any

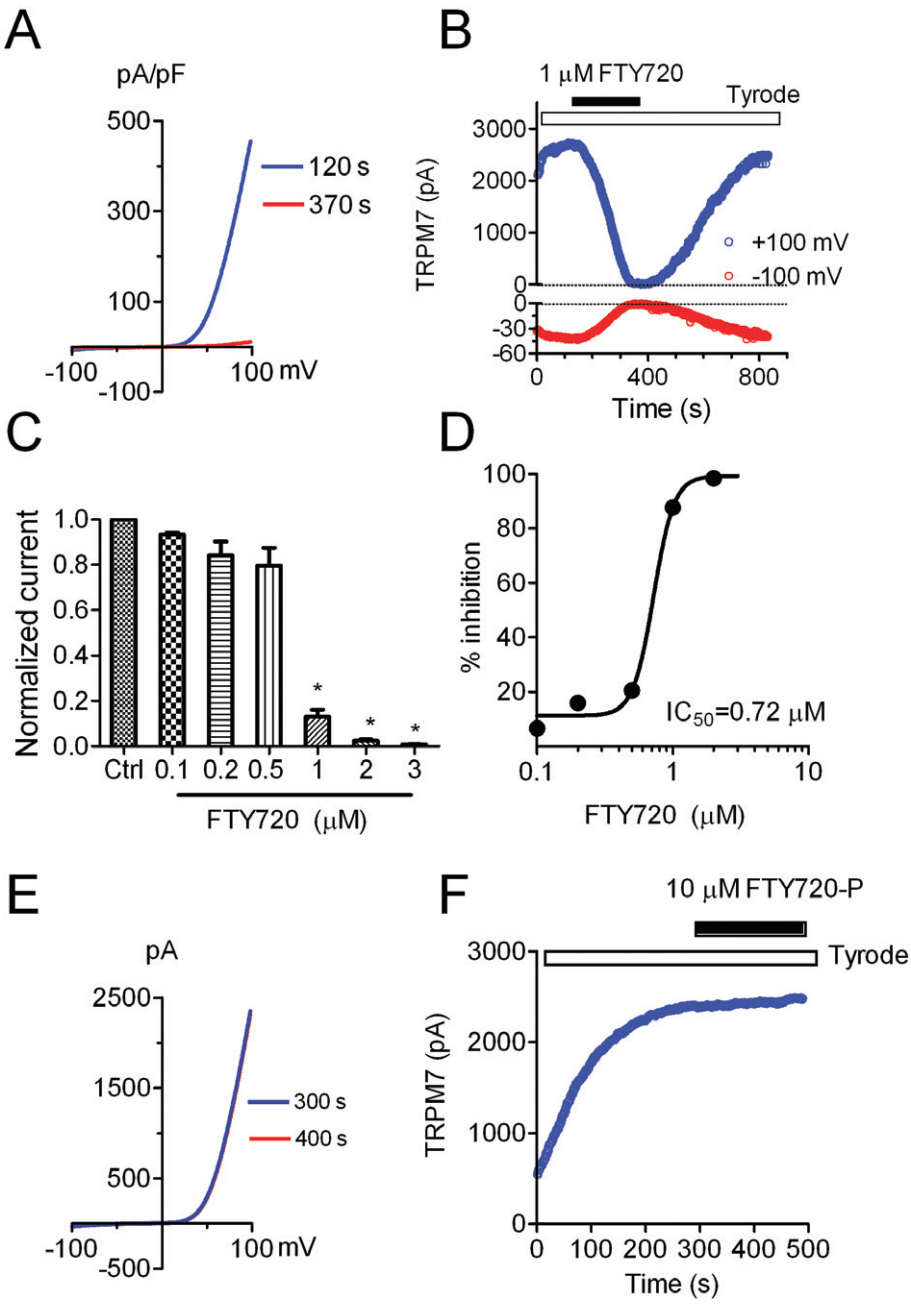

Figure 5

Effects of FTY720 and FTY720-P on TRPM7 channel activity evaluated by whole-cell current recording. (A) Blockade effects of 1 μM FTY720 on TRPM7 whole-cell current recorded in the HEK-293 cells over-expressing TRPM7. Current recorded at 120 s represents whole-cell current before FTY720 treatment, and current recorded at 370 s was after FTY720. (B) Time-dependent changes of TRPM7 outward current amplitude measured at +100 mV and inward current measured at –100 mV before and after 1 μM FTY720. Currents were completely blocked by 1 μM FTY720 and fully recovered after washout. (C) Inhibitory effects of FTY720 on TRPM7 at various concentrations (n = 4–6). (D) Dose–response curve of FTY720 on TRPM7. The average inhibition at each concentration of FTY720 was obtained by measuring the changes of current amplitude at +100 mV. Best fit of the dose–response curve yielded an IC_{50} of 0.72 ± 0.04 μM. (E) FTY720-P at 10 μM has no effect on TRPM7 currents. (F) TRPM7 current amplitude measured at +100 mV before and after 10 μM FTY720-P. Similar results were reproduced in another five cells.

effects on TRPM2 currents. However, TRPM2 currents were readily blocked by 30 μM ACA (Figure 11B). Figure 11C,D shows the effects of SPH on TRPM4 currents. TRPM4 currents were elicited by including 100 μM Ca^{2+} in the pipette solution (Figure 11C). NMDG-Cl was applied twice to ensure there was no leak current during the recording (Figure 11D). Application of 10 μM SPH did not alter inward or outward current amplitude of TRPM4. In order to study the effects of SPH on TRPM6 currents, we transfected TRPM6 plasmids into CHOK1 cells which have lower endogenous TRPM7 currents.

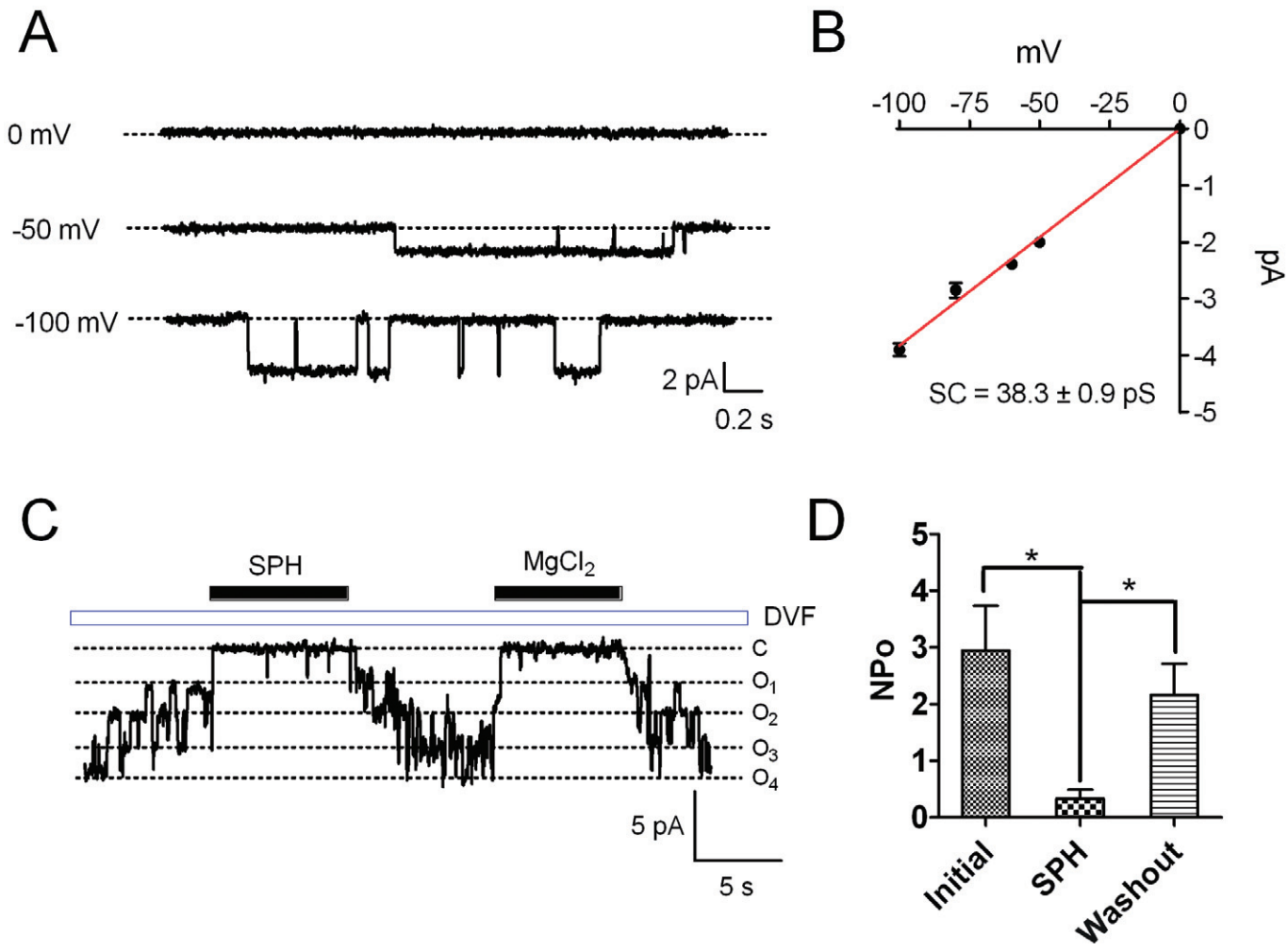

Figure 6

Effects of SPH on single-channel properties of TRPM7 recorded in HEK293 cells over-expressing TRPM7. (A) Single-channel current of TRPM7 recorded at different voltages in an inside-out excised patch. (B) Single-channel conductance of TRPM7. Linear regression of the single-channel current as a function of voltage yielded single-channel conductance of 38.3 ± 0.9 pS. (C) Effects of SPH on single-channel current. $MgCl_2$ (50 μM) was applied as a control in inhibiting TRPM7 current. (D) Average NP_o before and after application of SPH, and after washout.

TRPM6 currents were recorded using the same pipette solution for TRPM7 current recording (Figure 11E). Current amplitude was small in the beginning of the development of TRPM6 current (Figure 11E,F). To make sure the recorded current was TRPM6 but not TRPM7, we applied 200 μM 2-APB because it is known that 200 μM 2-APB inhibits TRPM7 but potentiates TRPM6 currents. As shown in Figure 11G, there was a significant increase in current amplitude after application of 200 μM 2-APB, indicating that the recorded current was indeed TRPM6 current. The effect of 2-APB was quickly reversed upon washout. When the current amplitude reached a steady state, 1 μM SPH was applied to the cell. TRPM6 current was markedly inhibited by SPH (Figure 11E–G). The IC_{50} of SPH block on TRPM6 was 0.46 μM, similar to the IC_{50} of SPH inhibition on TRPM7 currents. Like TRPM7, the recovery of TRPM6 from SPH block was very slow. The dashed traces in Figure 11E,F are representative traces of recovery after washout for 7 min. The results shown in Figure 11 suggest that the effect of SPH is relatively specific, as it only inhibits TRPM6, the closest homologue of TRPM7, but not other TRPM channels including TRPM2 and TRPM4.

Discussion

We demonstrate several new findings in this study. First, we found that SPH and FTY720 are potent inhibitors of TRPM7, whereas other ceramides, S1P and FTY720-P do not have any effect on TRPM7 channel activity. Second, it appears that SPH and FTY720 inhibit TRPM7 channel activity by reducing single-channel open probability. Third, SPH and FTY720 also potently block endogenous TRPM7 currents in cardiac fibroblasts. Fourth, blockade of TRPM7 in HEK-293 cells by FTY720 inhibits cell proliferation and migration, two cellular processes known to be influenced by TRPM7. Fifth, TRPM6, the closest homologue of TRPM7, is also blocked by SPH, whereas TRPM2 and TRPM4 are not altered by SPH. It is known that SPH is a potent bioactive sphingolipid which is involved in

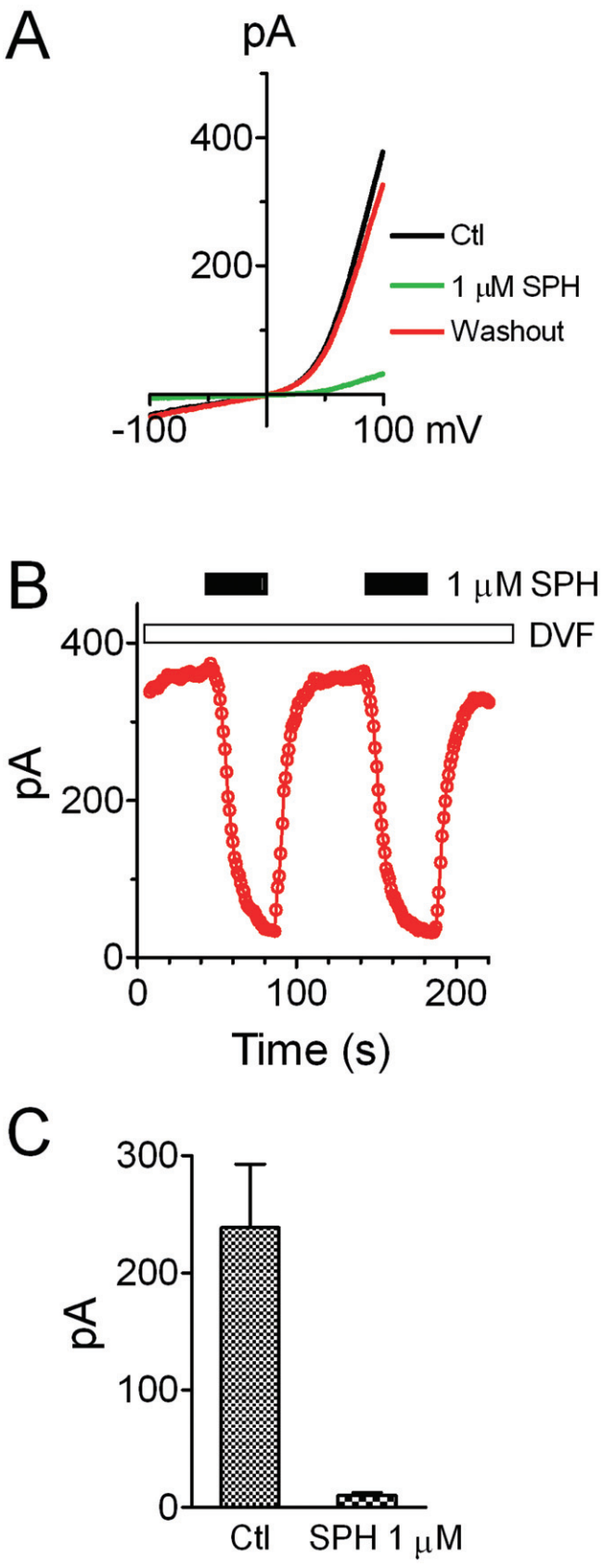

Figure 7

Effects of SPH on TRPM7 currents recorded by macropatches in HEK293 cells over-expressing TRPM7. (A) TRPM7 currents recorded in macropatches using a ramp protocol ranging from −100 to +100 mV. SPH at 1 μM applied in the bath solution (inside of the cell) completely inhibited TRPM7 currents. (B) Time-dependent changes of TRPM7 current amplitude (measured at +100 mV) before and after 1 μM SPH. The effects of SPH are reversible and reproducible. (C) Average TRPM7 current amplitude before and after 1 μM SPH ($n = 6$).

various biological processes, and that FTY720 is an immunosuppressant which has been used for multiple sclerosis treatment (Brinkmann, 2007; Brinkmann *et al.*, 2010). Although clinical efficacy of FTY720 is mostly mediated by convention to FTY720-P, mounting evidence suggests that FTY720 exerts *in vivo* and *in vitro* functions independent of S1PR pathways (Azuma *et al.*, 2003a,b; Pitman *et al.*, 2012). Given the inhibitory effects of SPH and FTY720, and the fact that TRPM7 is ubiquitously expressed in various types of cells and tissues, it is conceivable that TRPM7 may be a direct target of SPH and FTY720, thereby mediating S1P-independent physiological/pathological functions of SPH and FTY720.

SPH is a direct endogenous blocker of TRPM7

We demonstrate in this study that SPH is a strong inhibitor of TRPM7. SPH is an active lipid which can be readily converted to S1P by sphingosine kinase *in vivo* (Kohama *et al.*, 1998; Liu *et al.*, 2000). Although S1P could inactivate TRPM7 by depleting PIP_2 through activation of G_q-linked S1P receptors (Runnels *et al.*, 2002), several lines of evidence indicate that SPH blocks TRPM7 independent of S1P receptors. First, in HEK-293 cells over-expressing TRPM7, TRPM7 current was readily blocked by the low concentrations of SPH, FTY720 and DMS. However, S1P and FTY720-P did not block TRPM7, even at 10 μM, as HEK-293 cells do not express S1P receptors (Molderings *et al.*, 2007). Second, although SPH is a bioactive molecule which can activate signalling pathways such as phospholipase A_2 and phospholipase D (Spiegel and Milstien, 1996), we found that in inside-out excised patches, SPH and FTY720 completely blocked TRPM7 channel activity whereas S1P had no effect on single-channel currents. These results strongly indicate that SPH but not S1P is a direct inhibitor of TRPM7 which can block TRPM7 in the absence of other signalling molecules or pathways.

SPH is a potent inhibitor of TRPM7 and TRPM6

We demonstrate that SPH exhibits the most potent inhibitory effect on TRPM7. The IC_{50} of SPH or FTY720 for inhibiting TRPM7 current is in the sub-micromole range, while much higher concentrations are required for SPH to regulate other ion channels. For example, I_{CRAC} can only be completely blocked by 10 μM SPH and the IC_{50} of SPH to block I_{CRAC} is 6 μM (Mathes *et al.*, 1998). The IC_{50} of SPH on ryanodine receptors ranges from 10 to 40 μM (Sharma *et al.*, 2000). SPH also blocks cardiac Ca^{2+} and Na^+ currents (McDonough *et al.*, 1994; Yasui and Palade, 1996) and K^+ currents (Petrou *et al.*, 1994), as well as voltage-operated calcium channels in GH4C1 cells (Titievsky *et al.*, 1998). Although some channels

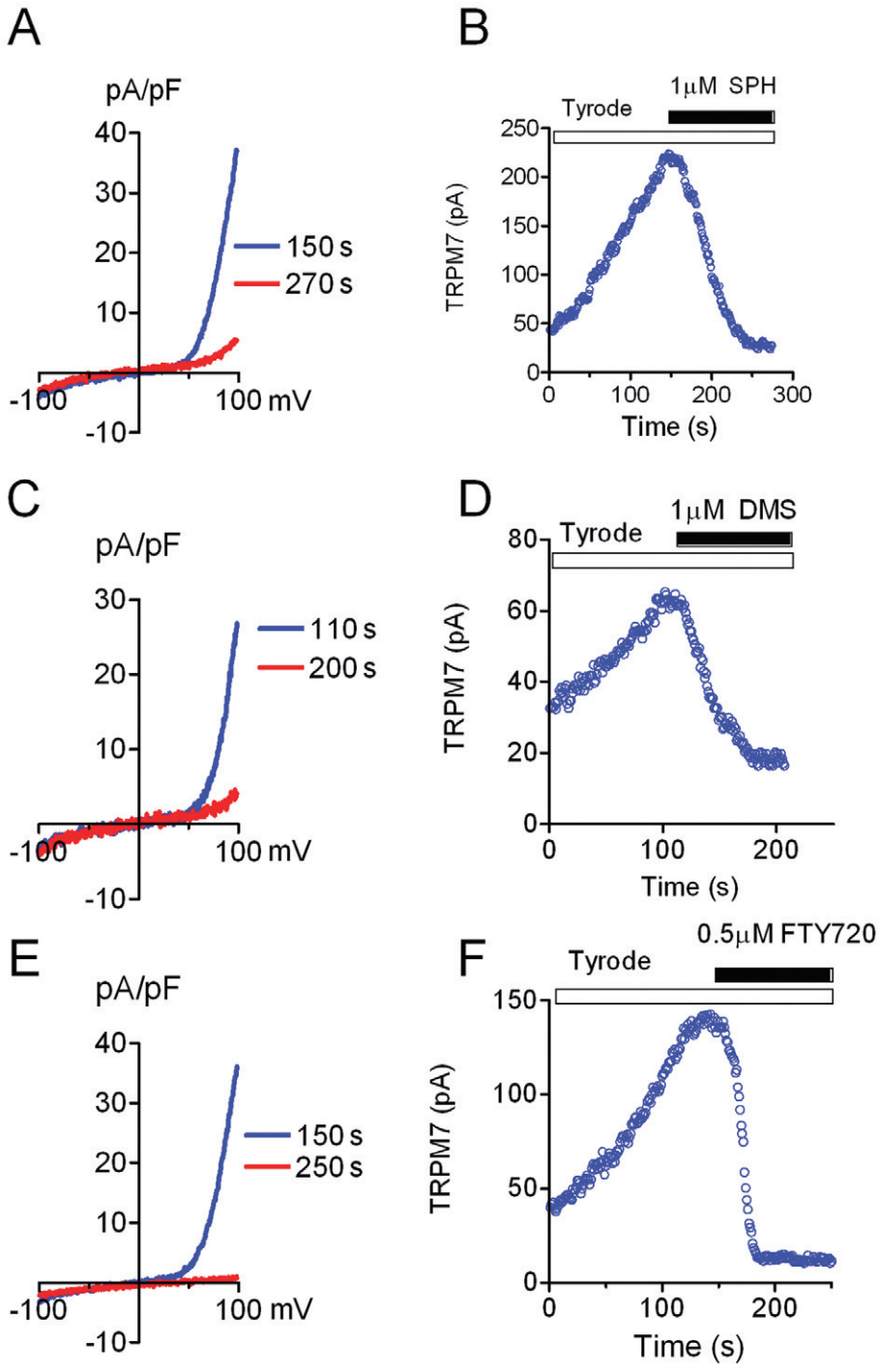

Figure 8

Effects of SPH, DMS and FTY720 on endogenous TRPM7 current in human atrial fibroblasts. (A, C, E) TRPM7 current elicited by a ramp protocol was blocked by 1 μM SPH (A), DMS (C) and FTY720 (E). (B, D, F) Changes of TRPM7 outward currents before and after application of SPH (B), DMS (D) and FTY720 (F).

are inhibited by SPH, Grimm and colleague found that SPH is an activator of TRPM3 (Grimm *et al.*, 2005). The concentration of SPH needed to induce half-maximal Ca^{2+} influx through TRPM3 is 12 μM (Grimm *et al.*, 2005). Interestingly, although TRPM3 can be activated by SPH, TRPC3, TRPC4, TRPC5, TRPV4, TRPV5, TRPV6 and TRPM2 did not respond to SPH application (Grimm *et al.*, 2005). We found that SPH can block TRPM6 with similar potency to TRPM7, but it has no effects on TRPM2 and TRPM4. Thus, the channel kinases TRPM6 and TRPM7 represent the first TRP channels known to

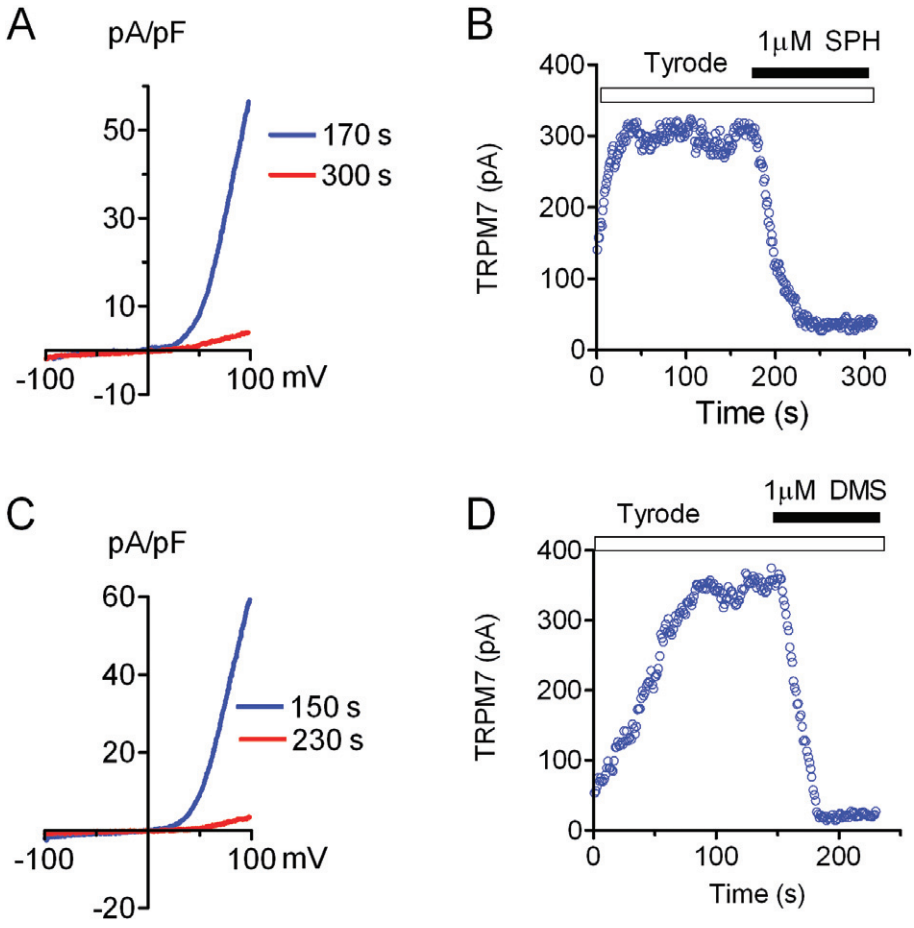

Figure 9

Inhibition of TRPM7 whole-cell currents by SPH and DMS in mouse cardiac fibroblasts. (A, C) TRPM7 currents before and after SPH (A) and DMS (C). (B–D) TRPM7 current amplitude before and after 1 uM SPH (B) and DMS (D). Similar results were obtained in five other fibroblasts.

be inhibited by SPH. Most importantly, it appears that SPH exerts the most potent inhibition on TRPM6 and TRPM7 in comparison to other ion channels shown to be blocked by SPH so far.

Mechanism by which SPH blocks TRPM7

We demonstrate that SPH and FTY720 inhibit TRPM7 by reducing channel open probability without changing single-channel conductance in inside-out patches (Figure 6). SPH blocks TRPM7 currents when applied in both extracellular (Figures 1, 4 and 5) and intracellular (Figures 6 and 7) sides. However, as SPH is a membrane permeable phospholipid, it is difficult to exclude its effects from either side. The effect of SPH on I_{CRAC} currents was reported to be mediated exclusively through inserting the SPH molecule to cell membrane, as intracellular application did not block I_{CRAC} (Mathes *et al.*, 1998). Unlike I_{CRAC}, the effect of SPH on a K^+ channel (Petrou *et al.*, 1994) is similar to that on TRPM7. SPH was shown to be able to block the K^+ single-channel currents in cell-attached configurations, as well as in excised patches from both inside-out and outside-out configurations (Petrou *et al.*, 1994). In contrast to the effects of SPH on I_{CRAC} (Mathes *et al.*, 1998), we found that the effects of SPH and FTY720 on TRPM7 in the inside-out excised patches can be easily and quickly washed out, suggesting that SPH and FTY720 may exert their effects from the cytosol side, but not by incorporating into the membrane. This is consistent with the notion that SPH is able to diffuse rapidly between cell membranes (Hannun *et al.*, 2001). Moreover, although the positively charged FTY720 and SPH potently inhibit TRPM7, their phosphorylated analogues FTY720-P and S1P do not have any direct effect on TRPM7, which could be due to the fact that the net positive charge is internally neutralized as the zwitterions in S1P and FTY720-P (Zheng *et al.*, 2006). We have previously reported that activation of TRPM7 requires the availability of PIP_2 (Runnels *et al.*, 2002; Xie *et al.*, 2011), and depletion of PIP_2 inactivates TRPM7. Moreover, it has been demonstrated that positive charge screening of PIP_2 inhibits TRPM7 activity (Kozak *et al.*, 2005). Thus, it is plausible that SPH and FTY720 inhibit TRPM7 channel activity by masking negative charges of PIP_2, thereby inactivating TRPM7 by reducing single-channel open probability.

Intracellular Mg^{2+} and Mg-NTPs have been demonstrated to play important roles in regulating TRPM7 channel functions (Demeuse *et al.*, 2006). Demeuse and colleagues demonstrated that the C-terminus truncation mutant of TRPM7 is

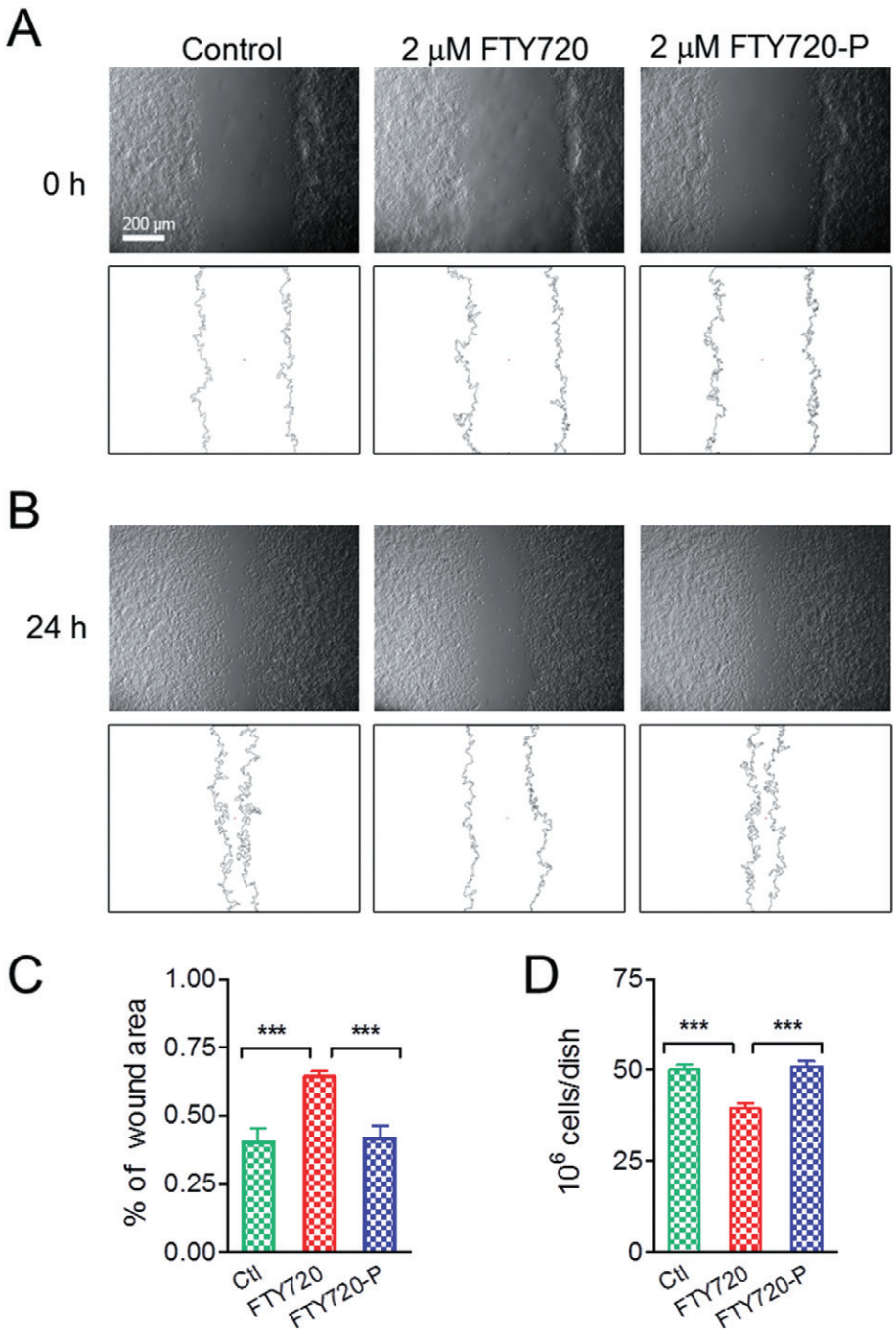

Figure 10

Effects of FTY720 on mobility and proliferation of HEK-293 cells. (A) Top: original images taken at 0 h after wounding in control, 2 μM FTY-720-treated and 2 μM FTY720-P-treated HEK-293 cells. Bottom: outlines of the wound determined using the program ImageJ. (B) Images taken 24 h after wounding (top), and outlines of the wound (bottom) in control, 2 μM FTY-720-treated and 2 μM FTY720-P-treated HEK-293 cells. (C) Average percentage of area closure assessed 24 h after wounding ($n = 6$, ***$P < 0.001$). (D) Effects of FTY720 and FTY720-P on proliferation of HEK293 cells over-expressing TRPM7. Cells were treated with control, 2 μM FTY720 and 2 μM FTY720-P for 48 h. Average data were from six independent experiments ($n = 6$, ***$P < 0.001$).

more sensitive to Mg^{2+}, and proposed that a Mg^{2+}-nucleotide binding site is at K1648 (Demeuse *et al.*, 2006). In two recent studies, it has been demonstrated that TRPM7 blockers Waixenicin A (Zierler *et al.*, 2011) and NS8593 (Chubanov *et al.*, 2012) block TRPM7 in a Mg^{2+}-dependent manner. As our experiments were conducted with Mg^{2+}-free pipette solutions, it seems that Mg^{2+} is not required for SPH and FTY720 to block TRPM7. Additionally, we found that the C-terminus truncation mutant of TRPM7 which lacks kinase domain (residues 1501–1863) was equally blocked by SPH (Supporting

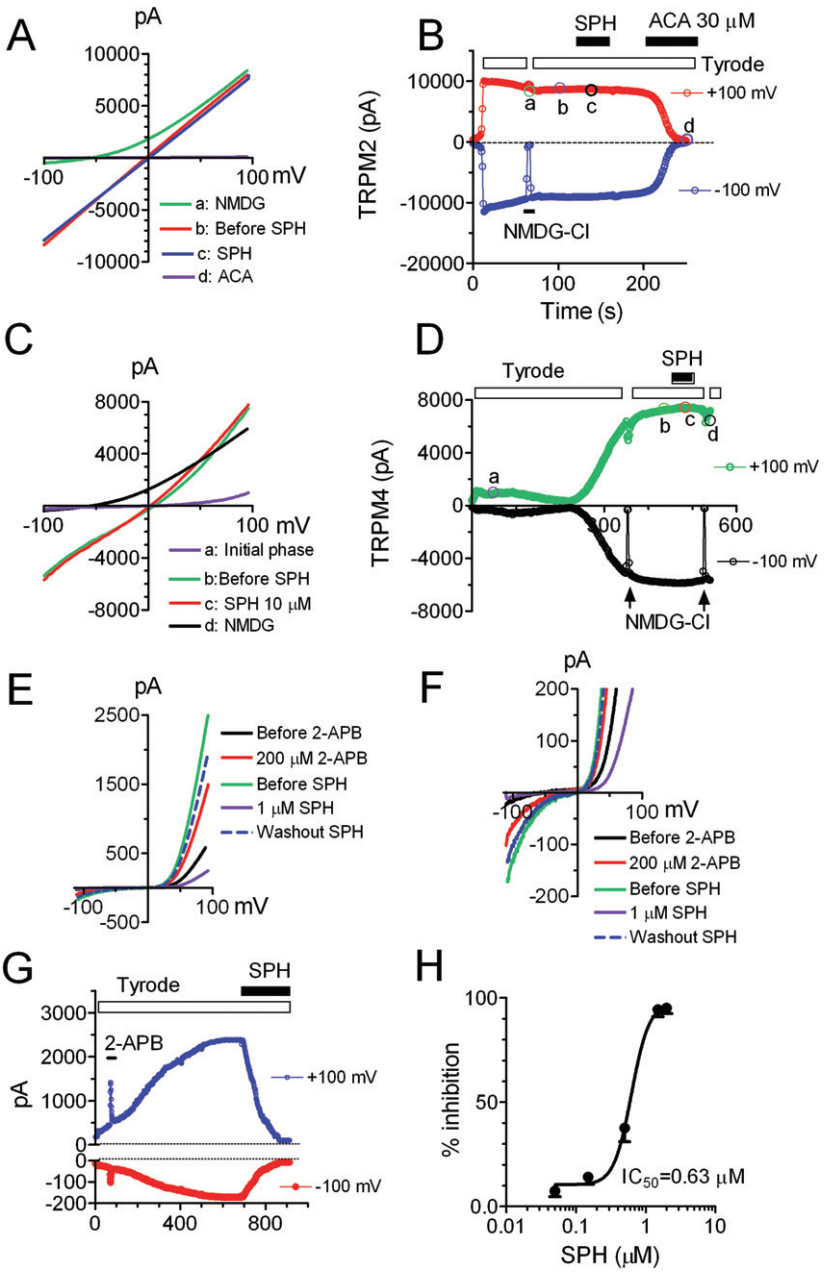

Figure 11

Effects of SPH on TRPM2, TRPM4 and TRPM6. (A–B) Effects of SPH on TRPM2 whole-cell currents recorded in HEK-293 cells. (A) Representative TRPM2 currents elicited by voltage ramps ranging from –100 to +100 mV under the following conditions: (a) when Tyrode solution was replaced by NMDG-Cl; (b) when current reached steady state (before SPH); (c) in the presence of SPH; (d) after block by 30 μM ACA. (B) Time-dependent changes of outward and inward currents of TRPM2 after replacement of Tyrode solution with NMDG (a), before (b) and after (c) 10 μM SPH, and in the presence of 30 μM ACA (d). NMDG was used to ensure that there were no leak currents. The time points labelled with 'a', 'b', 'c' and 'd' represent the time points when the representative recordings in 'A' were taken. (C–D) Effects of SPH on TRPM4 whole-cell currents recorded in HEK-293 cells by voltage ramp protocols. (C) Typical TRPM4 currents recorded after initial phase of activation (a), after second phase of activation, and when the current reached steady state (b) in the presence of 10 μM SPH (c), and with NMDG-Cl to replace Tyrode solution (d). (D) Time-dependent changes of outward and inward currents of TRPM4 in the absence and presence of 10 μM SPH. NMDG-Cl was applied twice to eliminate the possibility of involvement of leak currents. The time points labelled with 'a', 'b', 'c' and 'd' represent the time points when the representative recordings in 'C' were taken. (E–H) Effects of SPH on TRPM6 whole-cell currents. TRPM6 plasmids were transiently transfected into CHOK1 cells and the currents were elicited by voltage ramps ranging from –120 to +100 mV. (E) Typical TRPM6 recordings in the absence and presence of 200 μM 2-APB and 1 μM SPH, and after washout SPH. (F) Illustration of the changes in TRPM6 inward currents by the treatments shown in 'E'. (G) Time course of TRPM6 activation, potentiation by 2-APB, and inhibition by 1 μM SPH. The inward currents were measured at –100 mV and outward currents were measured at +100 mV. (H) Average inhibition of TRPM6 at various concentrations of SPH. The best fit of the dose–response curve yielded an IC_{50} of 0.63 ± 0.1 μM (n = 4–6 cells). Note that the effect of SPH was reversible. The dashed traces in (E) and (F) were recorded after washout for 7 min.

Information Fig. S2), suggesting that Mg^{2+}-nucleotide binding site K1648 is not necessary for SPH and FTY720-induced block on TRPM7. Nevertheless, further investigation is required to understand the detailed mechanism by which SPH and FTY720 inhibit TRPM6 and TRPM7.

Potential implications

TRPM7 exerts multiple cellular and physiological functions via its cation-permeable channel function and perhaps its kinase function (Aarts *et al.*, 2003; Schmitz *et al.*, 2003; Jin *et al.*, 2008; Ryazanova *et al.*, 2010; Low *et al.*, 2011; Middelbeek *et al.*, 2012). We demonstrated here that the bioactive phospholipids SPH and FTP720, but not the phosphorylated S1P or FTY720-P, potently blocked both inward and outward currents of TRPM7 (Figures 1 and 5), suggesting that inhibition of TRPM7 by SPH and FTY720 can generate cellular and physiological consequence. Indeed, HEK293 cells treated with FTY720 displayed significantly reduced proliferation and migration abilities (Figure 10). The concentrations of SPH and FTY720 needed to block TRPM7 are in the submicromolar range, similar to the plasma concentrations of S1P *in vivo* (0.19–0.7 μM) (Igarashi and Yatomi, 1998; Kihara *et al.*, 2007), and the concentrations of FTY720 for generating anticancer effects *in vivo* and *in vitro* (~2 to 10 μM) (Azuma *et al.*, 2003a,b; Lee *et al.*, 2005; Nagaoka *et al.*, 2008). The circulating concentration of SPH in plasma is in the nanomolar range (Knapp *et al.*, 2005), but the local concentration of SPH in cells and tissues can reach up to 268 μM (Arikawa *et al.*, 2002). SPH production can be increased by stimuli such as PDGF (Coroneos *et al.*, 1995) and apoptosis process (Suzuki *et al.*, 2004). The concentration of FTY720 for multiple sclerosis is at nanomolar levels, ranging from 35 to 53 nM for patients receiving the dosages of 1.25 and 5 $mg \cdot day^{-1}$ (Kovarik *et al.*, 2004). Therefore, it is likely that the SPH concentrations *in vivo* and the therapeutic concentrations of FTY720 for anti-cancer can effectively block TRPM7 currents.

FTY720 has two major functions: immunosuppressive effect and anti-cancer effect. Although the immunosuppressive effect is mainly mediated by FTY720-P through S1PRs, there are increasing amounts of evidence demonstrating that S1PR-independent effects play a major role in the anti-cancer function of FTY720 (Lee *et al.*, 2005; Nagaoka *et al.*, 2008; Pyne and Pyne, 2010). For example, it was demonstrated that FTY720, but not FTY720-P, was efficient in prevention of breast cancer metastasis in a mouse model (Azuma *et al.*, 2003b). Interestingly, it has been recently demonstrated that TRPM7 is required for breast cancer cell metastasis (Middelbeek *et al.*, 2012). It is promising that future investigations may reveal the potential link between the anti-cancer effects of FTY720 and its inhibitory effects on TRPM7.

In summary, this is the first study demonstrating that an endogenous signalling phospholipid, SPH, is a potent inhibitor of TRPM7. TRPM7 is a unique protein with both ion channel and protein kinase functions (Nadler *et al.*, 2001; Runnels *et al.*, 2001; Yamaguchi *et al.*, 2001). Although its physiological/pathological functions are still not fully understood, recent studies have revealed that TRPM7 is essential in a variety of physiological/pathological functions (Clapham, 2003; Runnels, 2010). Thus, understanding the inhibitory effects of SPH on TRPM7 may help towards a better understanding of the physiological and pathological functions of TRPM7. Moreover, like SPH, FTY720 can also potently inhibit TRPM7. Although FTY720 exerts its immunosuppressive effects through its active metabolite FTY720-P, FTY720 also exhibits direct effects on multiple signalling pathways (Xin *et al.*, 2007; Pyne and Pyne, 2010) as SPH does (Hannun and Obeid, 2008). Furthermore, we have previously demonstrated that activation of G_q-linked S1P receptors to deplete PIP_2 can completely inactivate TRPM7 in cardiac fibroblasts (Runnels *et al.*, 2002). Therefore, as a direct target of FTY720 and SPH, and an indirect target of S1P and FTY720-P via G_q-linked receptors, TRPM7 may serve as an important mediator of the physiological/pathological functions of SPH and FTY720, especially those independent of S1P signalling pathways.

Acknowledgements

We thank Drs. Loren Runnels and Andrew Scharenberg for providing us the HEK-293 cells stably expressing mTRPM7. We'd also like to thank Dr. Joost Hoenderop for providing us the TRPM6 construct, Dr. Yasuo Mori for providing us the TRPM2 construct, and Dr. Jean-Pierre Kinet for providing us the TRPM4 construct.

This work was generously supported by the National Institutes of Health, National Heart, Lung and Blood Institute (NHLBI) (http://www.nhlbi.nih.gov, Grant No. 2R01HL078960) to L. Y., and a bio-medical grant (Grant No. 2009-0099) from the Department of Public Health of Connecticut to L. Y.

Conflict of interest

None.

References

Aarts M, Iihara K, Wei WL, Xiong ZG, Arundine M, Cerwinski W *et al.* (2003). A key role for TRPM7 channels in anoxic neuronal death. Cell 115: 863–877.

Arikawa J, Ishibashi M, Kawashima M, Takagi Y, Ichikawa Y, Imokawa G (2002). Decreased levels of sphingosine, a natural antimicrobial agent, may be associated with vulnerability of the stratum corneum from patients with atopic dermatitis to colonization by Staphylococcus aureus. J Invest Dermatol 119: 433–439.

Azuma H, Horie S, Muto S, Otsuki Y, Matsumoto K, Morimoto J *et al.* (2003a). Selective cancer cell apoptosis induced by FTY720; evidence for a Bcl-dependent pathway and impairment in ERK activity. Anticancer Res 23: 3183–3193.

Azuma H, Takahara S, Horie S, Muto S, Otsuki Y, Katsuoka Y (2003b). Induction of apoptosis in human bladder cancer cells in vitro and in vivo caused by FTY720 treatment. J Urol 169: 2372–2377.

Bandhuvula P, Tam YY, Oskouian B, Saba JD (2005). The immune modulator FTY720 inhibits sphingosine-1-phosphate lyase activity. J Biol Chem 280: 33697–33700.

Bates-Withers C, Sah R (2012). Clapham DE TRPM7, the Mg(2+) inhibited channel and kinase. Adv Exp Med Biol 704: 173–183.

Berdyshev EV, Gorshkova I, Skobeleva A, Bittman R, Lu X, Dudek SM *et al*. (2009). FTY720 inhibits ceramide synthases and up-regulates dihydrosphingosine 1-phosphate formation in human lung endothelial cells. J Biol Chem 284: 5467–5477.

Brinkmann V (2007). Sphingosine 1-phosphate receptors in health and disease: mechanistic insights from gene deletion studies and reverse pharmacology. Pharmacol Ther 115: 84–105.

Brinkmann V, Billich A, Baumruker T, Heining P, Schmouder R, Francis G *et al*. (2010). Fingolimod (FTY720): discovery and development of an oral drug to treat multiple sclerosis. Nat Rev Drug Discov 9: 883–897.

Chen HC, Xie J, Zhang Z, Su LT, Yue L, Runnels LW (2010a). Blockade of TRPM7 channel activity and cell death by inhibitors of 5-lipoxygenase. Plos ONE 5: e11161.

Chen X, Numata T, Li M, Mori Y, Orser BA, Jackson MF *et al*. (2010b). The modulation of TRPM7 currents by nafamostat mesilate depends directly upon extracellular concentrations of divalent cations. Mol Brain 3: 38.

Chubanov V, Mederos y Schnitzler M, Meissner M, Schafer S, Abstiens K, Hofmann T *et al*. (2012). Natural and synthetic modulators of SK (K(ca) 2) potassium channels inhibit magnesium-dependent activity of the kinase-coupled cation channel TRPM7. Br J Pharmacol 166: 1357–1376.

Chun J, Brinkmann V (2011). A mechanistically novel, first oral therapy for multiple sclerosis: the development of fingolimod (FTY720, Gilenya). Discov Med 12: 213–228.

Clapham DE (2003). TRP channels as cellular sensors. Nature 426: 517–524.

Coroneos E, Martinez M, McKenna S, Kester M (1995). Differential regulation of sphingomyelinase and ceramidase activities by growth factors and cytokines. Implications for cellular proliferation and differentiation. J Biol Chem 270: 23305–23309.

Demeuse P, Penner R, Fleig A (2006). TRPM7 channel is regulated by magnesium nucleotides via its kinase domain. J Gen Physiol 127: 421–434.

Du J, Xie J, Yue L (2009a). Intracellular calcium activates TRPM2 and its alternative spliced isoforms. Proc Natl Acad Sci U S A 107: 7239–7244.

Du J, Xie J, Yue L (2009b). Modulation of TRPM2 by acidic pH and the underlying mechanisms for pH sensitivity. J Gen Physiol 134: 471–488.

Du J, Xie J, Zhang Z, Tsujikawa H, Fusco D, Silverman D *et al*. (2010). TRPM7-mediated Ca2+ signals confer fibrogenesis in human atrial fibrillation. Circ Res 106: 992–1003.

Elizondo MR, Arduini BL, Paulsen J, MacDonald EL, Sabel JL, Henion PD *et al*. (2005). Defective skeletogenesis with kidney stone formation in dwarf zebrafish mutant for trpm7. Curr Biol 15: 667–671.

Grigorova IL, Schwab SR, Phan TG, Pham TH, Okada T, Cyster JG (2009). Cortical sinus probing, S1P1-dependent entry and flow-based capture of egressing T cells. Nat Immunol 10: 58–65.

Grimm C, Kraft R, Schultz G, Harteneck C (2005). Activation of the melastatin-related cation channel TRPM3 [corrected] by D-erythro-sphingosine. Mol Pharmacol 67: 798–805.

Gwanyanya A, Sipido KR, Vereecke J, Mubagwa K (2006). ATP and PIP2 dependence of the magnesium-inhibited, TRPM7-like cation channel in cardiac myocytes. Am J Physiol Cell Physiol 291: C627–C635.

Hannun YA, Obeid LM (2008). Principles of bioactive lipid signalling: lessons from sphingolipids. Nat Rev Mol Cell Biol 9: 139–150.

Hannun YA, Loomis CR, Merrill AH, Jr, Bell RM (1986). Sphingosine inhibition of protein kinase C activity and of phorbol dibutyrate binding in vitro and in human platelets. J Biol Chem 261: 12604–12609.

Hannun YA, Luberto C, Argraves KM (2001). Enzymes of sphingolipid metabolism: from modular to integrative signaling. Biochemistry 40: 4893–4903.

Igarashi Y, Yatomi Y (1998). Sphingosine 1-phosphate is a blood constituent released from activated platelets, possibly playing a variety of physiological and pathophysiological roles. Acta Biochim Pol 45: 299–309.

Jiang J, Li M, Yue L (2005). Potentiation of TRPM7 inward currents by protons. J Gen Physiol 126: 137–150.

Jin J, Desai BN, Navarro B, Donovan A, Andrews NC, Clapham DE (2008). Deletion of Trpm7 disrupts embryonic development and thymopoiesis without altering Mg2+ homeostasis. Science 322: 756–760.

Jin J, Wu L-J, Jun J, Cheng X, Xu H, Andrews NC *et al*. (2012). The channel kinase, TRPM7, is required for early embryonic development. Proc Natl Acad Sci U S A 109: E225–E233.

Kerschbaum HH, Kozak JA, Cahalan MD (2003). Polyvalent cations as permeant probes of MIC and TRPM7 pores. Biophys J 84: 2293–2305.

Kihara A, Mitsutake S, Mizutani Y, Igarashi Y (2007). Metabolism and biological functions of two phosphorylated sphingolipids, sphingosine 1-phosphate and ceramide 1-phosphate. Prog Lipid Res 46: 126–144.

Kilkenny C, Browne W, Cuthill IC, Emerson M, Altman DG (2010). NC3Rs Reporting Guidelines Working Group. Br J Pharmacol 160: 1577–1579.

Knapp P, Dobrzyn A, Gorski J (2005). Ceramides, sphinganine, sphingosine and acid sphingomyelinases in the human umbilical cord blood. Horm Metab Res 37: 433–437.

Kohama T, Olivera A, Edsall L, Nagiec MM, Dickson R, Spiegel S (1998). Molecular cloning and functional characterization of murine sphingosine kinase. J Biol Chem 273: 23722–23728.

Kovarik JM, Schmouder R, Barilla D, Riviere GJ, Wang Y, Hunt T (2004). Multiple-dose FTY720: tolerability, pharmacokinetics, and lymphocyte responses in healthy subjects. J Clin Pharmacol 44: 532–537.

Kozak JA, Matsushita M, Nairn AC, Cahalan MD (2005). Charge screening by internal pH and polyvalent cations as a mechanism for activation, inhibition, and rundown of TRPM7/MIC channels. J Gen Physiol 126: 499–514.

Lahiri S, Park H, Laviad EL, Lu X, Bittman R, Futerman AH (2009). Ceramide synthesis is modulated by the sphingosine analog FTY720 via a mixture of uncompetitive and noncompetitive inhibition in an Acyl-CoA chain length-dependent manner. J Biol Chem 284: 16090–16098.

Lee MJ, Thangada S, Liu CH, Thompson BD, Hla T (1998). Lysophosphatidic acid stimulates the G-protein-coupled receptor EDG-1 as a low affinity agonist. J Biol Chem 273: 22105–22112.

Lee TK, Man K, Ho JW, Wang XH, Poon RT, Xu Y *et al*. (2005). FTY720: a promising agent for treatment of metastatic hepatocellular carcinoma. Clin Cancer Res 11: 8458–8466.

Li M, Jiang J, Yue L (2006). Functional characterization of homo- and heteromeric channel kinases TRPM6 and TRPM7. J Gen Physiol 127: 525–537.

Li M, Du J, Jiang J, Ratzan W, Su L-T, Runnels LW *et al.* (2007). Molecular determinants of Mg2+ and Ca2+ permeability and pH sensitivity in TRPM6 and TRPM7. J Biol Chem 282: 25817–25830.

Liu H, Sugiura M, Nava VE, Edsall LC, Kono K, Poulton S *et al.* (2000). Molecular cloning and functional characterization of a novel mammalian sphingosine kinase type 2 isoform. J Biol Chem 275: 19513–19520.

Liu W, Su LT, Khadka DK, Mezzacappa C, Komiya Y, Sato A *et al.* (2011). TRPM7 regulates gastrulation during vertebrate embryogenesis. Dev Biol 350: 348–357.

Low SE, Amburgey K, Horstick E, Linsley J, Sprague SM, Cui WW *et al.* (2011). TRPM7 is required within zebrafish sensory neurons for the activation of touch-evoked escape behaviors. J Neurosci 31: 11633–11644.

McDonough PM, Yasui K, Betto R, Salviati G, Glembotski CC, Palade PT *et al.* (1994). Control of cardiac Ca2+ levels. Inhibitory actions of sphingosine on Ca2+ transients and L-type Ca2+ channel conductance. Circ Res 75: 981–989.

McGrath J, Drummond G, McLachlan E, Kilkenny C, Wainwright C (2010). Guidelines for reporting experiments involving animals: the ARRIVE guidelines. Br J Pharmacol 160: 1573–1576.

McNeill MS, Paulsen J, Bonde G, Burnight E, Hsu MY, Cornell RA (2007). Cell death of melanophores in zebrafish trpm7 mutant embryos depends on melanin synthesis. J Invest Dermatol 127: 2020–2030.

Mandala S, Hajdu R, Bergstrom J, Quackenbush E, Xie J, Milligan J *et al.* (2002). Alteration of lymphocyte trafficking by sphingosine-1-phosphate receptor agonists. Science 296: 346–349.

Mathes C, Fleig A, Penner R (1998). Calcium release-activated calcium current (ICRAC) is a direct target for sphingosine. J Biol Chem 273: 25020–25030.

Middelbeek J, Kuipers AJ, Henneman L, Visser D, Eidhof I, van Horssen R *et al.* (2012). TRPM7 is required for breast tumor cell metastasis. Cancer Res 72: 4250–4261.

Molderings GJ, Bonisch H, Bruss M, Wolf C, von Kugelgen I, Gothert M (2007). S1P-receptors in PC12 and transfected HEK293 cells: molecular targets of hypotensive imidazoline I(1) receptor ligands. Neurochem Int 51: 476–485.

Nadler MJ, Hermosura MC, Inabe K, Perraud AL, Zhu Q, Stokes AJ *et al.* (2001). LTRPC7 is a Mg.ATP-regulated divalent cation channel required for cell viability. Nature 411: 590–595.

Nagaoka Y, Otsuki K, Fujita T, Uesato S (2008). Effects of phosphorylation of immunomodulatory agent FTY720 (fingolimod) on antiproliferative activity against breast and colon cancer cells. Biol Pharm Bull 31: 1177–1181.

Neviani P, Santhanam R, Oaks JJ, Eiring AM, Notari M, Blaser BW *et al.* (2007). FTY720, a new alternative for treating blast crisis chronic myelogenous leukemia and Philadelphia chromosome-positive acute lymphocytic leukemia. J Clin Invest 117: 2408–2421.

Parnas M, Peters M, Dadon D, Lev S, Vertkin I, Slutsky I *et al.* (2009). Carvacrol is a novel inhibitor of Drosophila TRPL and mammalian TRPM7 channels. Cell Calcium 45: 300–309.

Petrou S, Ordway RW, Hamilton JA, Walsh JV, Jr, Singer JJ (1994). Structural requirements for charged lipid molecules to directly increase or suppress K+ channel activity in smooth muscle cells. Effects of fatty acids, lysophosphatidate, acyl coenzyme A and sphingosine. J Gen Physiol 103: 471–486.

Pham TH, Okada T, Matloubian M, Lo CG, Cyster JG (2008). S1P1 receptor signaling overrides retention mediated by G alpha i-coupled receptors to promote T cell egress. Immunity 28: 122–133.

Pitman MR, Woodcock JM, Lopez AF, Pitson SM (2012). Molecular targets of FTY720 (fingolimod). Curr Mol Med [Epub ahead of print].

Prakriya M, Lewis RS (2002). Separation and characterization of currents through store-operated CRAC channels and Mg2+-inhibited cation (MIC) channels. J Gen Physiol 119: 487–507.

Pyne NJ, Pyne S (2010). Sphingosine 1-phosphate and cancer. Nat Rev Cancer 10: 489–503.

Runnels LW (2010). TRPM6 and TRPM7: a Mul-TRP-PLIK-cation of channel functions. Curr Pharm Biotechnol 12: 42–53.

Runnels LW, Yue L, Clapham DE (2001). TRP-PLIK, a bifunctional protein with kinase and ion channel activities. Science 291: 1043–1047.

Runnels LW, Yue L, Clapham DE (2002). The TRPM7 channel is inactivated by PIP(2) hydrolysis. Nat Cell Biol 4: 329–336.

Ryazanova LV, Rondon LJ, Zierler S, Hu Z, Galli J, Yamaguchi TP *et al.* (2010). TRPM7 is essential for Mg(2+) homeostasis in mammals. Nat Commun 1: 109.

Sahni J, Tamura R, Sweet IR, Scharenberg AM (2010). TRPM7 regulates quiescent/proliferative metabolic transitions in lymphocytes. Cell Cycle 9: 3565–3574.

Schmitz C, Perraud AL, Johnson CO, Inabe K, Smith MK, Penner R *et al.* (2003). Regulation of vertebrate cellular Mg2+ homeostasis by TRPM7. Cell 114: 191–200.

Sharma C, Smith T, Li S, Schroepfer GJ, Jr, Needleman DH (2000). Inhibition of Ca2+ release channel (ryanodine receptor) activity by sphingolipid bases: mechanism of action. Chem Phys Lipids 104: 1–11.

Spiegel S, Milstien S (1996). Sphingoid bases and phospholipase D activation. Chem Phys Lipids 80: 27–36.

Su LT, Agapito MA, Li M, Simonson WT, Huttenlocher A, Habas R *et al.* (2006). TRPM7 regulates cell adhesion by controlling the calcium-dependent protease calpain. J Biol Chem 281: 11260–11270.

Sun HS, Jackson MF, Martin LJ, Jansen K, Teves L, Cui H *et al.* (2009). Suppression of hippocampal TRPM7 protein prevents delayed neuronal death in brain ischemia. Nat Neurosci 12: 1300–1307.

Suzuki E, Handa K, Toledo MS, Hakomori S (2004). Sphingosine-dependent apoptosis: a unified concept based on multiple mechanisms operating in concert. Proc Natl Acad Sci U S A 101: 14788–14793.

Titievsky A, Titievskaya I, Pasternack M, Kaila K, Tornquist K (1998). Sphingosine inhibits voltage-operated calcium channels in GH4C1 cells. J Biol Chem 273: 242–247.

Vessey DA, Kelley M, Zhang J, Li L, Tao R, Karliner JS (2007). Dimethylsphingosine and FTY720 inhibit the SK1 form but activate the SK2 form of sphingosine kinase from rat heart. J Biochem Mol Toxicol 21: 273–279.

Xie J, Sun B, Du J, Yang W, Chen H-C, Overton JD *et al.* (2011). Phosphatidylinositol 4,5-bisphosphate (PIP2) controls magnesium gatekeeper TRPM6 activity. Sci Rep 1: 1–12.

Xin C, Ren S, Eberhardt W, Pfeilschifter J, Huwiler A (2007). FTY720 suppresses interleukin-1beta-induced secretory

phospholipase A2 expression in renal mesangial cells by a transcriptional mechanism. Br J Pharmacol 150: 943–950.

Yamaguchi H, Matsushita M, Nairn AC, Kuriyan J (2001). Crystal structure of the atypical protein kinase domain of a TRP channel with phosphotransferase activity. Mol Cell 7: 1047–1057.

Yasui K, Palade P (1996). Sphingolipid actions on sodium and calcium currents of rat ventricular myocytes. Am J Physiol 270 (2 Pt 1): C645–C649.

Zemann B, Kinzel B, Muller M, Reuschel R, Mechtcheriakova D, Urtz N *et al*. (2006). Sphingosine kinase type 2 is essential for lymphopenia induced by the immunomodulatory drug FTY720. Blood 107: 1454–1458.

Zheng W, Kollmeyer J, Symolon H, Momin A, Munter E, Wang E *et al*. (2006). Ceramides and other bioactive sphingolipid backbones in health and disease: lipidomic analysis, metabolism and roles in membrane structure, dynamics, signaling and autophagy. Biochim Biophys Acta 1758: 1864–1884.

Zierler S, Yao G, Zhang Z, Kuo WC, Pörzgen P, Penner R *et al*. (2011). Waixenicin A inhibits cell proliferation through magnesium-dependent block of transient receptor potential melastatin 7 (TRPM7) channels. J Biol Chem 286: 39328–39335.

Supporting information

Additional Supporting Information may be found in the online version of this article at the publisher's web-site:

Figure S1 Time course of SPH blockade on TRPM7. (A) The onset of 1 μM SPH block on TRPM7 is illustrated with an enlarged x-axis. The data in this panel are from the same recording shown in Figure 1D. (B) Superimposed time course of block by 0.5 and 1 μM SPH. Changes of currents at 0.5 and 1 μM SPH with time are shown as normalized currents to the maximal current amplitude of each concentration.

Figure S2 Effects of SPH on TRPM7 kinase truncation mutant (TRPM7-Trunc). Whole-cell currents were recorded in HEK-293 cells transiently transfected with TRPM7-Trunc plasmids. The TRPM7-Trunc was constructed by replacing the codon encoding serine 1501 with a stop codon. So the TRPM7-Trunc lacks residues 1501–1863. (A) Representative recordings of TRPM7-Trunc in the absence and presence of 1 μM SPH, as well as after washout. (B) Time-dependent changes of inward currents measured at −100 mV and outward currents measured at +100 mV before and after application of SPH. (C) Concentration-dependent effects of SPH on TRPM7-Trunc (n = 4–5 cells at each concentration). The IC_{50} obtained by the best fit of the dose–response curve was 0.46 ± 0.12 μM.